A Review of Selected Engineered Nanoparticles in the Atmosphere: Sources, Transformations, and Techniques for Sampling and Analysis

Brian J. Majestic,[1] Garnet B. Erdakos[†,2] Michael Lewandowski,[2] Karen D. Oliver,[3] Robert D. Willis,[2] Tadeusz E. Kleindienst,[2] and Prakash V. Bhave [2]

1 Department of Chemistry & Biochemistry, Northern Arizona University, Flagstaff, AZ 86011

2 National Exposure Research Laboratory, U.S. Environmental Protection Agency, Research Triangle Park, North Carolina 27711.

3 Alion Science and Technology, Box 12313, Research Triangle Park, NC 27709.

[†] NRC Postdoctoral Fellow

ABSTRACT

A state-of-the-science review was undertaken to identify and assess sampling and analysis methods to detect and quantify selected nanomaterials (NMs) in the ambient atmosphere. The review is restricted to five types of NMs of interest to the U.S. Environmental Protection Agency under their Office of Research and Development Nanomaterial Research Strategy: cerium oxide, titanium dioxide, carbon nanostructures (carbon nanotubes and fullerenes), zero-valent iron, and silver nanoparticles. One purpose is to determine the extent to which present-day ultrafine sampling and analysis methods may be sufficient for identifying and possibly quantifying engineered NMs (ENMs) in ambient air. Conventional sampling methods for ultrafines appear to require modifications. For cerium and titanium, background levels from natural sources make measurement of ENMs difficult to quantify. In cases where field studies have been performed, identification from only bulk analysis samples have been made. Further methods development is needed to identify these NMs, especially in specific size fractions of ambient aerosols.

Nanoparticles (NPs), which are defined as particles having at least one dimension < 100 nm [1], often possess different physical and chemical properties compared to their bulk-sized counterparts. Increased reactivity, strength, and conductivity at the nano-scale are key features leading to a boom in

production of nanomaterials (NMs), those materials with nano-scale morphology comprised of NPs or other nanocomponents. Sometimes, these differences can be attributed to increased surface area. However, in many cases, even the surface-area normalized reactivity of the NP is greater than that found in its bulk counterpart. In these instances, the increased reactivity may be due to surface defects (as with nano-cerium oxide) or the fact that particle size is approaching the quantum regime. [2]

NPs have become integral to the production of a variety of commercial products, such as sports gear, electronics, cosmetics, clothing, medicine, and food. [2-4] The Project on Emerging Nanotechnologies of the Woodrow Wilson International Center for Scholars maintains an online database designed to track the role of nanotechnologies and NMs in the production of consumer products (http://www.nanotechproject.org/inventories/consumer). A search of this database in February 2008 yielded 606 nanotechnology-based consumer products.[5] A subsequent search in September 2009 showed that the number of nanotechnology-based consumer products had nearly doubled, increasing to 1020. While this product survey is not authoritative, it does illustrate the increased use of NMs (68% increase in 19 months) and thus the greater potential for releases into the atmosphere. The intense interest surrounding NPs can also be seen from a research standpoint. From 1990 to 1999, approximately 4,000 articles were retrieved from the *Web of Knowledge* database using the search term "nanoparticles." The same search, performed in the date range January 2005 to September 2009, retrieved more than 67,000 articles. From a manufacturing standpoint, Meyer et al.[5] observed a sector-dependent increase in growth in production of products containing NMs—71% to 700% over a two-year period ending in 2008. These observations show the increased interest and importance of NPs in both the public and scientific communities. With the boom in NP production and lack of fundamental knowledge regarding their behavior in the air environment, NPs can truly be considered an emerging pollutant.[6]

The atmospheric aerosol community has long been investigating the composition and toxicity of ultrafine (UF) particles.[7, 8] However, until recently, most studies of UF particles have focused on incidental nanoparticles (INPs), that is, NPs created as byproducts of other processes. A large fraction of INPs in the atmosphere originate from combustion sources or freshly nucleated particles. The focus on

UF fractions (and therefore INPs) is, in large part, driven by the fact that these small particles can pose a danger to human health. Nano-sized particles can easily penetrate into the lower regions of the lungs and have been shown to enter the bloodstream through the CO_2/O_2 cardiopulmonary system exchange barrier.[2, 9] As a result, UF particles are linked with both respiratory and cardiovascular morbidity.[10-12]

The recent explosion in NM production has resulted in concerns about a new type of NP, the engineered nanoparticle (ENP). Unlike INPs, ENPs are intentionally produced for use in commercial products, as described above. With the expanding interest in and enormous economic potential for ENPs, it is likely that atmospheric emissions of these materials will increase.[13] As ENP production evolves into a more mature industry, it is essential to establish methods to quantify and characterize airborne ENPs both in occupational and environmental settings.

Since research on ENPs in the atmosphere has yet to be undertaken to a substantial degree, and presently there are few ENP-specific sampling techniques, an examination of the measurement methods for UF particles (diameter < 100 nm) represents a first step for selecting methods for ambient ENP measurements. UF measurements are generally performed by collecting samples using filter- or impactor-based techniques followed by off-line analytical measurements, and typically reported as air concentrations in terms of mass per volume of air passing through the collection medium, usually as μg m^{-3}. However, mass measurements may significantly underrepresent the importance of particles < 100 nm. For example, Figure 1 (adapted from Kittelson et al.[14]) shows the mass and number distribution of particles collected from diesel engine exhaust. In terms of particle mass, three modes are observed: nuclei, accumulation, and coarse modes. However, on the basis of particle number, only the nuclei mode is important to a significant degree. In this light, substantial work has recently been performed to determine the size distribution of NPs rather than their overall mass. The details of these and other considerations have driven the measurement methods reviewed in this paper.

The U.S. Environmental Protection Agency has recently formulated a Nanotechnology White Paper to consider policy implication of the use of NMs and its Nanomaterial Research Strategy develops a strategic plan to understand sources of and exposures to NMs.[15] One of the initial activities in the plan has

been to examine the applicability of present-day measurement techniques to ENPs released into the atmosphere. Measurements aimed at elucidating the sources and potential impacts of ENPs could be confounded by background concentrations of INPs, especially in ambient UF particles. Understanding the techniques likely to be applicable for measuring and quantifying NMs in ambient air initially requires an understanding of the sources, properties, and potential transformations of these compounds in real world airsheds to provide adequate requirements for precision and accuracy of candidate methods.

This review presents the state-of-the-science of sampling and analysis (currently considered to be applicable to UF particles in ambient air) of five selected NMs: cerium oxide, titanium dioxide, carbon nanostructures (carbon nanotubes and fullerenes), zero-valent iron, and silver NPs. A primary goal of this review is to determine the extent to which present-day techniques used to characterize UF particles are applicable to the sampling and analysis of ENPs. While the review focuses on work found in traditional peer-reviewed journal articles, information was also drawn from communications with current investigators, as well as reports prepared by industry and government agencies.

We begin with a description of known sources, properties, and potential transformations of the selected NMs to provide context for the measurement methods being considered. Next, sampling techniques for UF particles (and NPs by extension) are reviewed, followed by current analytical and characterization techniques. Lastly, we summarize results from relevant field measurements. An appendix of acronyms has been provided as a convenience to the reader, as well as for cases where first use descriptions prove to be awkward.

Sources, Properties, and Transformations of Engineered Nanoparticles in the Atmosphere

NPs are released into the environment by natural mechanisms and through anthropogenic routes. The increased production of NMs may lead to an increased concentration of these materials in the air. To understand the impact of ENPs on human health exposures and deposition to ecosystems, and also to place this review in context, it is important to understand their potential sources of release into the

atmosphere, their physical and chemical characteristics, and possible transformations once emitted. The factors discussed in this section will address several or all of the following topics for each NM: (1) the origin of NPs emitted into the atmosphere (engineered or incidental, natural or anthropogenic), (2) the chemical and physical nature of the NPs, (3) the potential physicochemical transformations of the NPs upon release, and (4) potential effects of the NPs on physicochemical transformations of other atmospheric species. Information on the sources of the NPs considered in this review is summarized in Table 1.

nano-Ceria (n-ceria; n-CeO_2)

Cerium is the most abundant rare-earth element in the earth's crust, with an average concentration of 50 ppm.[16] Reff et al.[17] recently reported anthropogenic emissions of 69.3 tons yr^{-1} of cerium in $PM_{2.5}$ (particulate matter with diameter ≤ 2.5 μm) in the U.S., and identified seven corresponding source categories. Mass fractions of cerium in all seven source categories fall below 0.6%. In the form of cerium oxide (CeO_2), major commercial uses of the compound include flint material, glass polish and decolorizer, and as a catalyst for control of vehicle emissions, either as a thin washcoat in three-way catalytic converters in gasoline engines or as a fuel-borne catalyst (FBC) in diesel engines.[18, 19] Applications also exist in other industrial processes,[16] solar cells,[20] and fuel cells.[21] The most likely potential source of n-ceria in the ambient atmosphere would be from its use as a FBC. We, therefore, focus on this source here.

There are presently three diesel fuel additive products that contain nano-sized cerium as a FBC: (1) Eolys™, manufactured by Rhodia Electronics & Catalysis, based in France; (2) Envirox™, originally manufactured by Oxford-based Oxonica Energy Limited, and now owned by Energenics Pte Ltd.; and (3) Platinum Plus®, from Clean Diesel Technologies, based in the U.S. Of these, only Platinum Plus® is currently registered with the EPA for use in on-road diesel vehicles in the United States. Because all contents of Platinum Plus® and Envirox™ are already listed on the Toxic Substances Control Act

(TSCA) Chemical Substance Inventory, both can be used for off-road diesel applications in the U.S. While all three of these additives contain nano-scale cerium (5-7 nm in primary particle size), the specific formulation of each is proprietary and confidential business information. Nevertheless, some details are public knowledge. Eolys™ (particularly the DPX-9 formulation) has been reported to contain n-CeO_2 dispersed in an organic solvent,[22] Envirox™ contains n-CeO_2, which is described as being dispersed in an aliphatic/cycloaliphatic hydrocarbon fluid with the aid of dispersants,[23] and Platinum Plus® contains a nanocrystallite cerium product comprised of a colloidal mixture of amorphous and crystalline cerium hydroxide, which is transformed into n-ceria upon combustion.[24]

The primary purpose of n-ceria FBCs is to catalyze the oxidation of soot, resulting in reduced diesel particulate matter (DPM) emissions and increased fuel economy. Unlike ceria on the micron scale, n-ceria has been shown to contain a large number of surface defects. These defects are primarily a result of oxygen vacancies in its crystal structure.[25] As a result of these defects, molecular oxygen is easily adsorbed to the surface, and thus n-ceria is a powerful oxidation catalyst. As the vacancies become filled with oxygen, the oxygen becomes available to oxidize soot at temperatures more than 200°C below the temperature at which soot would otherwise be oxidized. During the process of soot oxidation, the oxygen trapped in the vacancies oxidizes the soot and the n-ceria becomes reduced. Oxygen can then be readsorbed and the process can continuously cycle.[26]

The oxidation of diesel soot and corresponding reduction of particulate carbon emissions by cerium-based fuel additives has been demonstrated in several studies.[27-31] Although these additives reduce DPM emissions on a mass basis, studies have also shown that they can cause significant increases in number concentrations of particles in the nuclei mode illustrated in Figure 1 (that is, particles with mobility diameters < 50 nm).[22, 32] This shift in particle size distribution, which becomes more pronounced as the additive concentration in fuel is increased, may be the result of at least two different processes: (1) the oxidation of soot may lead to increased concentrations of volatile organic compounds (VOCs) that could form nuclei mode particles, and (2) homogeneous nucleation of n-ceria. Imaging and chemical analysis of the resulting nuclei mode particles indicates that they are predominantly composed of n-

ceria.[22, 32] Jung et al.[22] found that n-ceria can be emitted in diesel exhaust in two ways: (1) "decorating" the surface of larger soot agglomerates, and (2) as aggregates of n-ceria. It is important to note that in both of these cases, the size of the n-ceria is 5-7 nm.

No studies have yet been published on the fate of n-ceria FBCs once emitted into the atmosphere. However, one study has determined that n-ceria has the ability to efficiently reduce hydrogen peroxide, a common atmospheric constituent generated as a chain-terminating product of the self reaction of hydroperoxyl radicals in the atmosphere.[33] Another study showed that n-ceria both decarboxylates and polymerizes some small organic molecules.[34] Therefore, it is expected that emissions of n-ceria could impact transformations of other atmospheric species.

nano-Titania (n-titania; n-TiO_2)

Numerous consumer products, such as paints, cosmetics, and sunscreens, contain n-titania for its pigmentary, photocalytic, and UV protective properties.[5, 35, 36] n-Titania is also receiving attention for its photocatalytic properties in air purification and water treatment applications.[37-41] Release of n-titania from the majority of applications summarized above will be to aquatic environments, however, TiO_2 has been detected in the ambient atmosphere.[42-44] Total anthropogenic emission of $PM_{2.5}$ titanium in the U.S. is reported to be 14,400 ton y^{-1}.[17] Sources of n-titania in the atmosphere could include aerosolization from water treatment processes, paint wear, and wind-blown crustal material. Titanium is the ninth-most abundant element in Earth's crust, and n-titania has been observed in the lungs of ancient humans, including the Tyrolean ice man (a 5,300 year-old mummy found preserved in alpine glacier ice).[45] While mechanisms of release to the atmosphere have not received much attention, airborne release of n-titania in manufacturing plants has been investigated. During the manufacturing process, titania is primarily released during material handling.[46] Employees in the manufacturing sector are most susceptible to inhalation of ENPs of titania.

TiO_2 is a semiconductor with a low band-energy, < 385 nm for anatase and < 400 nm for rutile

(two of the three crystalline forms of TiO_2), leading to strong photolytic properties. As with n-ceria, titania is capable of participating in both reduction and oxidation reactions. This is accomplished by producing electron hole pairs, as shown below:[47]

$$TiO_2 \xrightarrow{h\nu} e^-_{eb}(TiO_2) + h^+_{vb}(TiO_2)$$

Several investigators have found that, compared to rutile, anatase is the more photoactive form of titania.[48-50] In fact, Jang et al. determined that the crystalline form of titania was a more important parameter than particle size in the decomposition of bacteria and ammonia.[48] Additionally, titania was found to deactivate n-heptane for at least 30 hours without losing activity.[51] By contrast, after a 15 h interaction period with SO_2, titania lost activity as a photocatalytic agent which was likely due to SO_3 adsorbed onto the surface. However, the catalyst was found to be easily regenerated by sonication in deionized water.[51]

After TiO_2 is emitted to the atmosphere, it catalytically oxidizes nitric oxide (NO) to form nitrogen dioxide (NO_2) and oxidizes organic molecules to form CO_2,[37] which has implications with respect to how particulate titania can interact with other atmospheric species and promote the formation of ozone (O_3). For example, the presence of uncoated rutile (anatase was not examined) allowed the photooxidation of propan-2-ol to occur at a rapid rate.[52] When coated with > 1% (w/w) silica, the oxidation of propan-2-ol decreased and eventually terminated at approximately 16% silica (w/w). This likely occurred due to an increased silica concentration on the surface of the titania blocking any resulting photoactivity.[52] This is relevant to atmospheric systems because a significant portion of crustal-derived aerosols are composed of silica.[53, 54] Thus, it is possible that titania may be quickly deactivated in arid areas with high concentrations of wind-blown dust. Clearly, additional studies would be required to confirm this hypothesis.

Carbon Nanoparticles – Carbon Nanotubes and Fullerenes

Carbon NPs are common in the atmosphere in at least three forms: (1) carbon nanotubes (CNTs), (2) fullerenes, and (3) soot. All of these may be present as INPs produced by combustion of hydrocarbons. We briefly summarize combustion sources of carbon-based INPs only to provide context for studies on ENPs. Soot agglomerates, such as those found in diesel exhaust, are primarily carbonaceous and are produced from the incomplete combustion of hydrocarbons. It is estimated that 25% of the particulate carbon in diesel exhaust is amorphous soot while the other 75% is comprised of CNTs and fullerenes.[55] Other incidental sources of CNTs and fullerenes include methane, propane, and natural gas combustion streams.[56] As for carbon-based ENPs, CNTs have been found to be one of the most promising materials in nanotechnology for energy storage and composite materials, among other applications.[57] Fullerenes, and derivatives thereof, have been studied extensively for applications in solar cells, chemical sensors, drug delivery, bacterial and viral inhibition, and antioxidant activity.[58] Although CNTs and fullerenes accounted for a quarter of available NMs included in the Nanowerk LLC online database in 2009,[5] airborne sources have not been investigated outside of exposures in manufacturing facilities. Potential sources of these ENPs in the atmosphere include release during incineration of industrial and medical solid waste, as well as treatment of liquid waste, as described for silver NPs by Quadros and Marr.[59] Engineered CNTs and fullerenes are produced using several different methods and may contain trace amounts of various contaminants such as yttrium and nickel, which are often used as catalysts in the synthesis of these NMs.[60] The presence of these contaminants could distinguish ENPs from INPs.

CNTs may exist as single-wall carbon nanotubes (SWCNTs) or multi-wall carbon nanotubes (MWCNTs). SWCNTs can be thought of simply as one-atom-thick sheets of graphite (called graphene) rolled into tube-like structures that are typically 1–2 nm in diameter and can have lengths up to several millimeters. MWCNTs are modeled as concentric tubes or as a graphene sheet rolled around itself. CNTs have many unique properties that can be "tuned" by varying their diameter, length, and chirality: 1) they have the largest tensile strength and elasticity of all known materials; 2) they can act as conductors, semiconductors, or superconductors; and 3) they are excellent thermal conductors. Like CNTs, fullerenes

are pure carbon structures, but are cage-like rather than tube-like. The first fullerene discovered (buckminsterfullerene, i.e., C_{60}) resembles its namesake's geodesic domes as well a soccer ball. Variations of these "buckyballs" consist of structures such as C_{20} and C_{70}. Fullerenes have been considered to be the most efficient radical scavengers and have actually been described as "radical sponges".[61] Fullerene C_{60} has been shown to exhibit the quantum behavior of wave-particle duality.[62] Although fullerenes are hydrophobic, they can be functionalized to become water-soluble and capable of carrying drugs and genes for delivery to cells.

Unlike fullerenes and CNTs, which have high degrees of crystallinity, soot is a highly amorphous entity.[45, 55, 63] Typical NTs in a combusted-methane air stream averaged 20 nm in diameter, with aggregates about 2 μm long composed of several thousand NTs.[55] Aggregates in a propane combustion stream had a similar diameter and were on the order of 1.5 μm long. In most aqueous and organic solvents, pure CNTs tend to aggregate due to van der Waals forces, forming rope-like structures.[64]

Although a significant amount of work has gone into understanding the atmospheric chemistry of carbon NPs, there is still considerable uncertainty in interpreting experimental observations. For example, investigators have concluded that O_2 and N_2 in the atmosphere will adsorb onto SWCNTs.[65, 66] However, using CNTs and pristine "buckypaper" (essentially a macroscopic film of CNTs), Goldoni found that these adsorption properties disappeared after contaminants contained in the carbon matrix were removed.[67] Several studies have examined oxidation reactions of fullerenes in the gas phase, and have demonstrated influence by temperature, oxidizing species, and specific fullerene structure. These have shown that, while exposure of crystalline C_{60} to pure O_3 at room temperature and heating in ambient air at 250 °C produced no detectable oxides, a mixture of C_{60} (90%) and C_{70} (10%) exposed to O_2 in air at 300 °C produced a mixture comprised of 33% by mass oxygen, and a C:O molar ratio ~100 times lower than that of pure C_{60}.[68, 69] Both C_{60} and C_{70} exposed to room-temperature O_2 containing 6.4% by volume O_3 yielded formation of CO_2 gas and ketonic groups on the fullerenes.[70] An average fullerene composition of $C_{60}O_{8.6}$ resulted from mechanical stress applied to crystalline C_{60} in a pure O_2 atmosphere for several hours.[71] Investigations of physicochemical transformations of CNTs and fullerenes with other

atmospheric species were not found in the literature.

Zero-Valent Iron (ZVI)

Iron is the fourth-most abundant element in Earth's crust, and typically exists as iron oxide compounds in the +2 (ferrous) and +3 (ferric) oxidation states. According to Reff et al.[17], total $PM_{2.5}$ iron emissions in the U.S. are 103,000 ton yr^{-1}. NPs of zero-valent iron, i.e., metallic iron (Fe^0), have received considerable attention for application in remediation of contaminated groundwater and soil.[72] While this application will not likely lead to appreciable releases of ZVI NPs to the atmosphere, ferrocene, an organometallic iron compound, is one of three most-used cetane enhancers in diesel fuel in the U.S. and Canada, and has been considered as a diesel fuel additive to reduce emissions of DPM.[73, 74] The iron in ferrocene is normally assigned an oxidation state of +2, but is emitted as NPs of iron oxides or ZVI in diesel exhaust when combusted in diesel fuel.[74] As a result, the primary route of ZVI NPs emitted to the atmosphere is from the combustion of ferrocene in diesel engines.

ZVI NPs as used in remediation applications are commonly represented by a core-shell model in which metallic iron comprises the core, and iron oxides and hydroxides form the shell.[72] These NPs thus exhibit characteristics of both forms of iron acting as sorbents and reductants. Upon combustion of ferrocene-additized diesel fuel, ZVI NPs form when vaporized iron in the diffusion flame self-nucleates in cooler regions outside the flame.[74] In existing studies where ferrocene was doped into diesel fuel, ZVI NPs (ca. 5-10 nm) were imaged in the exhaust. Similar to cases with n-ceria, the ZVI NPs were found in metallic aggregates ranging from 20 to 200 nm and as single particles decorating carbon agglomerates.[74–77]

Once released to the atmosphere, ZVI has been shown to be very unstable. Upon exposure to molecular oxygen, ZVI reacts to form Fe(II) and hydrogen peroxide. Once Fe(II) is formed, Fenton chemistry dominates, resulting in Fe(III) and additional hydrogen peroxide.[78, 79] After 1 h in pure water, ZVI is transformed completely to magnetite (Fe_3O_4) and lepidocrite (α-FeOOH).[80] Upon oxidation to

Fe(II) or Fe(III), reactive oxygen species (ROS) are produced, which may react with organic or sulfur compounds in the atmosphere. ZVI has also been shown to react with oxalate, another important atmospheric constituent, forming oxidized iron and hydroxyl radicals.[79]

Silver Nanoparticles (Ag NPs)

The U.S. emissions inventory of silver in $PM_{2.5}$ is 157 ton yr^{-1}, according to Reff et al.[17] In 2009, Ag NPs were used in half of all consumer products included in the Project on Emerging Nanotechnologies' online database.[5] They are most commonly used as antimicrobial and antibacterial agents and are added to products including detergents, clothing, medical devices and supplies, water purifiers, personal care products, and air filters.[36, 59, 81, 82] In their review of environmental and human health risks of airborne silver NPs, Quadros and Marr[59] estimate that, during use, about 14% of these products have potential to release silver particles into air. They describe releases that may occur into indoor air (during production/manufacturing and domestic use) and the ambient atmosphere through pathways such as spraying, dispersion, and waste disposal as noted previously for CNTs and fullerenes.

Due to their low solubility and high reactivity, some silver NPs are "capped" with stabilizing agents (e.g., surfactants, ligands, and polymers) during synthesis to prevent particle aggregation and control particle size.[36, 59, 81, 83] Some products described by manufacturers as silver NPs may actually be silver colloids,[36] but product details are often confidential. Considering the range of products containing Ag NPs, unknown details about pathways of release into air, and a limited number of measurements of airborne Ag, little can be said about specific physical and chemical characteristics. One study of Ag NP agglomerates generated by evaporation and condensation of a 99.999% silver powder reported agglomerate aspect ratios of 1.77 ± 0.56, 1.71 ± 0.51, and 1.79 ± 0.51 for mobility diameters of 80, 120, and 150 nm, respectively, as well as an average primary particle size of 13.8 ± 2.5 nm.[84] Shin et al.[84] also summarize data from other studies on Ag NP agglomerates in which average primary particle sizes ranged from 13-20 nm. Quadros and Marr[59] generated silver NPs that had a median diameter of 32.4 nm.

Ag NP aerosols have also been generated in numerous inhalation toxicology studies, and those employing nebulizers have produced particles with aerodynamic diameters as small as 5 nm.[59]

Upon release of Ag NPs to the atmosphere, a number of physicochemical transformations of the NPs and other airborne species could potentially occur. Examples include agglomeration of Ag NPs, aggregation with larger particles, coating of the NPs by organic matter, dissolution into cloud or fog droplets, and chemical reactions with atmospheric oxidants.[59] The adsorption of SO_2 to Ag NPs in solution and of various organic compounds to substrates of Ag NPs used in surface enhanced Raman spectroscopy (SERS) studies has been observed.[81] Aside from a study demonstrating that Ag NPs in contact with ambient air tarnish rapidly,[85] other data on airborne transformations were not found.

Sampling Techniques for Atmospheric Nanoparticles

Most sampling techniques used for the collection of NPs are based on methods previously developed for the collection of UF particles. While these UF particle sampling methods, such as filter collection and impactor sampling, can often be successfully adapted to the collection of ENPs, a number of complicating factors have been observed with the use of such methods. For example, an examination of a traditional impactor sampling device adopted for use with NP collection revealed several potential complicating factors: (1) The high pressure drop produced in the impactor sampler could potentially disrupt NP agglomerates. Such disruption might not significantly affect bulk analysis methods (e.g., ICP-MS, EC-OC, total mass) but could severely compromise single-particle imaging techniques (e.g., TEM, SEM).[86] (2) Particle bounce from the supermicron stages during impactor sampling may have a large relative effect on bulk analyses in the NP size range.[86] (3) Due to their low density, the aerodynamic size of carbon agglomerates is generally much smaller than their mobility diameter equivalent. This leads to a much higher concentration of particles below 100 nm collected in the impactor sampler relative to a mobility measurement.[87, 88]

Factors such as these can potentially affect other UF sampling methods adopted for the sampling

of NPs. While they may be mitigated by various modifications, strict quality assurance controls are generally required to minimize potential sampling artifacts. In some cases, investigators have begun to examine the use of less traditional sampling methods, such as techniques focused on electrical charging or thermal deposition, in order to better preserve the morphological properties of airborne NPs.

NP sampling methods can be broadly divided into two classes: bulk sampling methods and size-classified sampling methods, most of which are included in Table 2. Bulk sampling methods, such as filter sampling, can be of considerable value for occupational sampling or source sampling studies, where NP concentrations tend to be high. For atmospheric sampling, however, where background concentrations of INPs or ambient PM can be significantly higher than the concentrations of ENPs of interest, bulk sampling techniques tend to be less valuable and the use of size-classified sampling methods, such as impactor samplers, is often required.

Bulk Sampling Devices. Filter sampling is among the most widely used methods for the sampling of fine and UF particles. From the perspective of atmospheric sampling of NPs, the primary disadvantage of filtration is the fact that a relatively broad size fraction is collected on the filter media, making it difficult to differentiate ENPs from other collected particles. However, many ambient PM monitoring networks already make use of filter-based samplers, which tends to encourage the development of analytical methods that can detect NPs collected on filters. In addition, many of the archived samples available from previously conducted field campaigns consist primarily of filter samples, so retrospective analyses of ENPs will likely need to contend with bulk filter samples.

The non-size selective nature of filter samples can be dealt with in a number of different ways. One common approach is to couple filter sampling with a single-particle analytical technique, such as electron microscopy (discussed in more detail in the Analytical Techniques section), which is capable of picking out NPs of interest from a more complex mixture. For example, Chianelli et al.[54] collected particles in Mexico City using a high-volume sampler, then suspended the filter in an ultrasonic bath containing isopropanol. A single drop of suspension was then placed on a TEM grid for analysis. They

obtained particles in the nanometer range (average 40 nm) and found crystalline nano-structures containing silicon, iron, and manganese. Peters et al. used low-volume (4 L min^{-1}) respirable filter-based samplers to collect particles on mixed cellulose ester (MCE) filter media.[89] The MCE filter media were prepared for analysis by collapsing them in a water-dimethyl formamide-glacial acetic acid mixture as described by Burdett and Rood.[90, 91] Han et al.[92] used another type of low-volume sampler (1.5 L min^{-1}) to collect particles on MCE filters in a MWCNT manufacturing facility. Using NIOSH Method 7402, the investigators affixed the filters to a TEM grid for analysis.

The limitations inherent in non-size selective filter samples can also be mitigated to some extent through experimental design. For example, Park et al.[93] developed a sampling campaign intended to examine cerium oxide emissions from the use of n-ceria diesel fuel additives. Ambient PM_{10} samples were collected both before and after the introduction of doped fuel to a local bus fleet. Even though the sampling relied on non-size selective filter samples and bulk analytical techniques, an appreciable increase in cerium concentrations was detected and attributed to n-ceria emissions from the combustion of the doped diesel fuels. While this filter sampling approach did not provide details regarding the size, structure, or morphology of the cerium particles, it did serve as an effective screening technique.

One alternative to filter sampling that is of considerable interest for NP sampling is electrostatic precipitation. Unlike impaction and some filter sampling techniques, electrostatic precipitation is a low-pressure sampling method in which artificially charged NPs are attracted to an oppositely charged electrode. It is estimated that the kinetic energy of particles in the electrostatic precipitator is about 10 times less than in a low-pressure impactor, reducing the breakup of agglomerates.[84] Furthermore, electrostatic precipitation has shown collection efficiencies of >99% for particles less than 100 nm.[94] However this reported high efficiency is in contrast to a laboratory-constructed device described by Miller et al.[74] Several investigators have employed electrostatic precipitation with applications ranging from roadway dust to biological molecules.[48, 95] Carbon nanofibers and diesel exhaust have been collected directly onto TEM grids using electrostatic precipitation.[74, 96] Dahl et al.[95] used this device to collect tire-wear particulate matter.

A number of related techniques may also allow for particle collection without substantial pressure drops. Photoelectric charging (PC) and diffusion charging (DC) have been used for sampling of fine and UF particles, and may be suitable for use with NPs as well. In the photoelectric charging technique, particles are exposed to UV radiation so that they emit photoelectrons. The electrons attach to the oxygen in the air and form a negatively charged ion. The resulting positively charged particle is guided by an electric field to an electrode and the particle number concentration is measured relative to the current at the electrode. This method has been successful for the detection of particulate polyaromatic hydrocarbons (pPAHs) less than 1μm.[97, 98] In diffusion charging, particles are exposed to a charged gas stream which are then collected at an electrode. Like the PC technique, particle number is obtained relative to the electric current produced.[98] In combination with PC, DC has been used to identify combustion sources (e.g., diesel soot, cigarette smoke).[97]

One additional family of sampling methods thought to be potentially useful for preserving the structure of NP aggregates is thermal precipitation or thermophoretic precipitation (TP). In the TP technique, the sampler uses a heated tungsten wire and a cooled copper block to guide the particles directly to a TEM grid. The particles are thermally driven to the cold copper TEM grid where they can be directly analyzed. The collection efficiency of the TP is nearly 100% for particles less than 100 nm.[42] For soot aggregates, Zhang and Megaridis contend that the TP is ideal because it preserves the morphological state of the aggregates.[76] Many investigators[45, 56, 76, 99, 100] use the TP to collect directly onto the TEM grid. However, Shi et al.[87] have shown that Teflon filters can also be used. In addition, Ku and Maynard[96] used a TP device for collection and characterization of Ag NP aggregates.

Size-Classifying Sampling Devices. Size classifying sampling devices, which collect one or more narrowly-bounded particle size fractions onto suitable media, can be particularly useful for ambient atmospheric sampling, since highly complex mixtures of particles with size distributions ranging from the nanometer to supermicron size ranges are common. The use of size classifying sampling devices helps remove potential sampling biases introduced by particles that are not in the size range of interest, which

allows a wider range of analytical methods to be employed. In particular, the use of size-classification at the sampling stage can allow chemical characterization and quantification of NPs to be performed with lower-cost, higher throughput bulk analytical methods.

One of the more widely examined size-classifying sampling methods available is impactor sampling. Impactor samplers divide particulate matter into a series of different size fractions by impacting smaller and smaller particles as the flow is passed over a substrate. Generally, size segregation is achieved by passing the air through sequentially smaller nozzles or slits. Impactor samplers allow investigators to easily collect various size fractions of aerosols using a single sampler. One common impactor sampler is the micro-orifice uniform-deposit impactor (MOUDI). When combined with the nano-MOUDI, this device size segregates aerosols into 15 fractions with size cuts at: 18, 10, 5.6, 3.2, 1.8, 1.0, 0.56, 0.32, 0.18, 0.1, 0.056, 0.032, 0.018, and 0.010 μm.

Fang et al.[101] used a nano-MOUDI to measure the size-distribution of NPs near a roadway. They used sealed covers to minimize volatilization and reaction with atmospheric gases following collection. Grose et al.[102] collected particles smaller than 320 nm using a nano-MOUDI for chemical and gravimetric analysis. The issue of particle bounce was addressed by greasing the impactor plates in the supermicron fractions so the large particles stick to the plates rather than bounce into the nano-fraction size range. Ntziachristos et al.[103] used a MOUDI/nano-MOUDI to collect particles near a freeway in Los Angeles. The MOUDI was modified by plugging two-thirds of the inlet holes. Consequently, the airflow was reduced to 10 L min^{-1} (from 30 L min^{-1}). While the motivation for plugging the holes was not explicitly stated, presumably, a decrease in the kinetic energy of the incoming particles led to a reduction in particle binding and agglomerate breakup. In comparison to the distribution from a Scanning Mobility Particle Sizer (SMPS), the size distribution using the nano-MOUDI yielded an R^2 value of 0.84 and a slope of 1.07, implying little difference between the two techniques for ambient particles.

One of the main drawbacks of the MOUDI impactor is the high flow rate and associated high pressure drop, which, as discussed earlier, can lead to certain sampling artifacts. Low-volume impactors (LVI) and low-pressure impactors (LPI) are intended to reduce or remove these artifacts. By reducing

airflow through the impactor, Fushimi et al.[104] have reported that particle bounce is negligible. Low-volume impactors (e.g., Dekati Ltd., Tempere, Finland), which separate aerosols into 15 fractions, with size cuts at 10; 6.5; 4; 2.4; 1.6; 0.98; 0.62; 0.38; 0.25; 0.15; 0.10; 0.055; 0.028; and 0.007 μm, are commercially available. Fujitani et al.[105] utilized the Sioutas personal cascade impactor sampler (PCIS) operating at 9 L min^{-1} to measure the size distribution of aerosol in a titanium dioxide manufacturing facility. The ratio of the personal sampler to the SMPS in the fine fractions was somewhat higher than that observed by Ntziachristos et al.[103] for the MOUDI/SMPS pairing, ranging from 1.1 to 1.3. These relatively small differences indicate that low-volume impactor samplers are candidates for use in NP sampling.

LPIs have been used by several investigators for collection of NPs.[74] Lee et al.[75] used a LPI in a study that measured the metal content in diesel exhaust, but the sampling details (i.e., flow rate, substrate) were noted to be available in a future study. Using a LPI, Miller et al.[74] collected aerosol samples greater than 50 nm directly onto a TEM grid for subsequent analysis. However, Shi et al.[88] hypothesize that electrical LPI (ELPI) samplers overestimate particle volume due to particle fractal properties.

Another widely used size-classifying sampling device is the electrostatic classifier. The electrostatic classifier uses a charged electrode to separate particles based on their electrical mobility. By screening for a specific mobility range, the electrostatic classifier continuously produces a monodisperse aerosol. The most common electrostatic classifier is the differential mobility analyzer (DMA). The standard DMA can generate monodisperse particle distributions with mobility diameters of as little as 10 nm. The nano-DMA can separate particles down to a mobility diameter of 2 nm.[106] The monodisperse aerosols generated by the DMA are commonly analyzed with particle counters to evaluate particle size distributions. However, the DMA output may also be directed into other sampling devices, such as an electrostatic precipitator. At least one commercial electrostatic precipitation sampler is available from TSI, Inc. (St. Paul, MN; Model 3089: Nanometer Aerosol Sampler). In a personal communication, however, Jennerjohn reported that the collection efficiency of the Model 3089 was negligible when collecting particles in a CNT research laboratory.[107]

Another device developed previously for fine and UF particle sampling that is being evaluated for use with NPs is the parallel-flow diffusion battery (PFDB). The PFDB uses cells of increasing diffusion length in parallel to each other (as opposed to a serial flow diffusion battery) and arranged such that the same air flow rate passes through each cell of the instrument and each cell samples the input aerosol (Cheng and Yeh[108]; Cheng et al.[109]). Aerosol exiting each cell can be collected independently on filters or TEM grids for determining the chemical composition and/or particle morphology in each size fraction. Barr et al.[110] employed a seven-cell PFDB operated at a flow rate of 14.7 L min^{-1} to determine the size distribution of diesel exhaust, oilshale dust, and carbon black coated with benzo(a)pyrene. Particles smaller than 0.7 μm were classified into eight size bins by the PFDB.

Analytical Techniques for Characterization of Atmospheric Nanoparticles

General Overview

The techniques reviewed in this section have been used to characterize NP samples collected in laboratory, occupational, or atmospheric settings and are subdivided into three main categories: (1) real-time particle size determination, (2) chemical analyses of bulk samples, and (3) single-particle analyses. The primary tool for determination of particle size distributions is a scanning mobility particle sizer (SMPS), which has been used extensively for particle analysis under a variety of conditions. The bulk analyses covered here are primarily concerned with determining the chemical composition of a sample. Most have been used previously for the analysis of UF particles, and have been more recently evaluated for use with NMs under laboratory conditions or for occupational sampling. These techniques include elemental carbon and organic carbon (EC-OC) analysis and a number of spectroscopic techniques, such as inductively coupled plasma mass spectrometry (ICP-MS), atomic absorption spectroscopy (AAS), and X-ray fluorescence spectroscopy (XRF). Many single-particle analysis techniques have been extensively used to examine NMs under laboratory conditions, and these techniques are increasingly being used to

examine NP constituents in occupational and atmospheric samples. While many single-particle analysis techniques require sample collection prior to analysis (e.g., SEM, TEM, EDS, ED), several real-time single-particle analysis methods are also available, including single-particle mass spectrometry (SPMS) and nanoaerosol mass spectrometry (NAMS). Details of the operation of some of these techniques are provided below, along with examples of their applicability to the evaluation of atmospheric samples. The analytical techniques are also summarized together with some salient features in Table 3.

Particle Size Distribution

Scanning Mobility Particle Sizer (SMPS). Twenty years after its development, the SMPS is still the most common method many investigators use to measure aerosol size distributions.[75, 95, 102, 111-118] The SMPS is a two-component device that contains (1) an electrostatic classifier and (2) a particle counter. The electrostatic classifier produces a monodisperse aerosol that is sent to the particle counter. By scanning a series of different size fractions in sequence and counting the resulting particles, an overall particle size distribution can be obtained. The most common electrostatic classifier is the differential mobility analyzer (DMA). Commercially available DMAs are capable of producing monodisperse aerosols down to 10 nm (standard DMA) or 2 nm (nano-DMA).[106] Investigators have used various forms of the SMPS in several settings, including ambient sampling[112, 119] and laboratory studies.[96, 102, 120, 121] While the SMPS in not very effective in analyzing ENPs in the atmosphere, due to the complex nature of ambient aerosols, it can be a very useful tool in occupational settings or in the evaluation of specific ENP sources.

Engine Exhaust Particle Sizer (EEPS) & Fast Mobility Particle Sizer (FMPS) Spectrometers. The EEPS and FMPS can be used to measure the size distribution of aerosols emitted from sources, such as engines, where the particle distribution changes rapidly with time.[105, 115, 122] Similar to the SMPS, size separation is achieved with the use of a DMA. Whereas the SMPS uses a fixed slit and a single detector (a particle counter) to scan and quantify the particle distribution, the EEPS and FMPS use a series of electrometers

(one per size channel) spaced along the axial dimension of the charging rod, thus acting as a spectrometer to a mixed ensemble of particles. The advantage of this approach compared to the SMPS is a considerably improved time resolution, of up to two orders of magnitude for the EEPS. Thus for engine operation, the particle size distribution can be determined at various stages of engine operation (e.g., for the Federal Test Procedure). For cases where particle changes are slow with time, the SMPS has the advantage of using a detector with considerably higher sensitivity. Like the SMPS, the EEPS and the FMPS are most effective as laboratory tools for the evaluation of potential NP emission sources.

Bulk Analyses

Inductively Coupled Plasma–Mass Spectrometry (ICP-MS). ICP-MS is a powerful analytical tool used in environmental elemental analysis of soils, water, and air. ICP-MS uses a plasma to ionize a sample dissolved in a weakly acidic solution. ICP-MS can be used to detect iron, titanium, cerium, and silver, but cannot be used to detect CNTs or fullerenes. The primary strength of ICP-MS is that very low detection limits can be achieved (<1 ppt for most elements using high resolution). The primary weakness of ICP-MS is that information contained in the sample regarding structure and agglomeration is lost during the digestion. This can be partially overcome by utilizing a reliable size-resolved sampler. ICP-MS may become increasingly important because it is currently unclear if the adverse health effects of CNTs are a result of the NT or of the metals contained within the NT[57, 75]. Another weakness of ICP-MS is the requirement for a sample to be in aqueous form, which frequently constitutes an extra analytical step. For difficult digestions, as is the case with CNTs,[57] highly-trained personnel are generally required.

One application of ICP-MS in current NP research is the determination of total metal content in NPs collected near limited-access freeways.[103] In addition, investigators measured the residual catalysts in CNTs to better understand toxicity and explored the use of Y:Ni ratios to identify CNTs.[107, 123]

Atomic Absorption Spectroscopy (AAS). AAS is a venerable technique that quantitatively measures the elemental composition of metals in aqueous solutions. Concentrations of the target analyte are proportional to the amount of light absorbed by the sample (using Beer's Law) after being vaporized by an acetylene flame (FAAS) or in a graphite furnace. Although AAS has been largely supplanted by other analytical techniques, such as ICP-MS, it is still in use in a number of analytical laboratories. For example, Fang et al.[101] used FAAS to measure NP concentrations in air after collection using a nano-MOUDI sampler.

Elemental Carbon / Organic Carbon Analysis (EC-OC). EC-OC is measured using a carbon analyzer. There are two approaches for conducting this measurement. One method used in the IMPROVE monitoring network collects aerosol on quartz filter media.[124] Following collection, OC is measured by heating the aerosol to 500 °C in an inert atmosphere (usually helium). The elemental carbon, which consists primarily of soot, fullerenes, and CNTs, is measured by heating the residual aerosol to up to 800 °C in a 2% oxygen stream. A similar approach, referred to as the STN method, uses a somewhat different temperature program and means of detection. The ease of use makes this technique attractive. If used in parallel with a size-segregated sampling technique, the EC values can provide an estimate of carbon-based NPs. However, this technique cannot distinguish between CNTs, fullerenes, and diesel soot.

Using EC-OC, Fushimi et al. observed that the OC/EC ratio decreases with particle size in particulate matter collected near a roadway.[104] This finding indicates that nucleation of organic particles may be a mechanism of NP production in this setting. Fujitani et al.[105] distinguished carbon ENPs from INPs using EC-OC measurements in a nanocarbon production facility.

Fluorescence. Studies have shown that CNTs undergo fluorescence in the near-IR range. The energy of the fluorescence is dependent on at least two parameters: the chirality and the tube length.[125–128] This specificity makes fluorescence a potentially valuable tool for characterization of CNTs. If the CNT is present as an agglomerate, however, the fluorescing photon may be quenched by the neighboring carbon

atoms. As a result, much of the light may never reach the detector. Therefore, while this technique may be useful for the characterization of CNTs, it is likely to be unsuitable for CNT quantification.[129]

X-ray Fluorescence (XRF). XRF spectroscopy measures the elemental concentrations directly from a solid sample. The sample is bombarded by high-energy X-rays, and the lower energy X-rays emitted from the sample, which are specific to an element, are measured. XRF has been used by investigators to measure the elemental composition of fine fibers collected from the atmosphere.[54]

X-ray Absorption Spectroscopy (XAS). XAS includes techniques such as X-ray absorption near-edge structure (XANES) spectroscopy and extended X-ray absorption fine structure (EXAFS) spectroscopy. XAS techniques use a focused X-ray beam (usually from a synchrotron source) to exploit subtle differences in excitation energy based on the oxidation state and bonding environment of the target analyte. XAS is useful for NP analysis in two ways: (1) to directly measure the oxidation state or chemical speciation of the NP or (2) to directly measure how a pollutant transforms in the presence of the NP.

Chen et al.[47] utilized XANES spectroscopy to measure how n-titania behaves in the presence of the common pollutants copper and mercury. Using Ti, Cu, and Hg XANES, the authors observed that n-titania was able to effectively reduce Cu(II) to Cu(0) and Hg(II) to Hg(0). EXAFS spectroscopy has been employed to identify platinum NPs emitted from a diesel engine.[130]

Single-Particle Analyses

Scanning Electron Microscopy (SEM) & Transmission Electron Microscopy (TEM). SEM is a very common electron microscopy imaging technique. When using SEM, an electron beam is focused onto the sample and the secondary electrons emitted from the sample are detected. SEM creates a 2-D image, with

a spatial resolution on the high-end instruments as good as 1–2 nm.[129] SEM can be used to image any type of NP, as long as the size is sufficiently large. A host of authors have used SEM in order to directly observe NPs in ambient and laboratory settings.[89]

While SEM is suitable to detect NPs in most situations, analysis of particles approximately 1 nm or less requires the use of TEM. Although analysts have been using TEM for decades to image atmospheric particles, it is quickly becoming one method of choice for characterizing airborne NPs. During TEM analysis (which is more like an optical microscope than SEM), the electron beam passes through the sample. Here, an image is created on a screen behind the sample. Using TEM, a resolution of ~ 0.05 nm can be obtained with the higher-end instruments.[131] TEM analysis is not restrictive in terms of potential analytes. CNTs, fullerenes, silver, ZVI, and ceria have been observed on a TEM. Like SEM, the major drawbacks of TEM are that (1) they require highly trained technicians and (2) only a small fraction of the sample is typically analyzed, leaving open the possibility that the analyzed area is not representative of the sample. Environmental TEM (ETEM) can also be used to measure how NPs behave in different gases outside of a vacuum.[132] Similar to SEM, TEM is an extremely common analytical tool for observing NPs. A host of authors have used TEM in order to directly observe NPs in ambient and laboratory settings.[45, 54, 89, 95, 117]

Energy Dispersive Spectroscopy (EDS) & Electron Energy Loss Spectroscopy (EELS). EDS (or energy dispersive X-ray spectroscopy [EDX]) utilizes the X-rays produced from the sample during TEM or SEM analysis. As each element emits X-rays at a unique energy, elemental maps can be created for individual particles. EDS, or EDX, is useful for detecting and quantifying elements present in the sample.

TEM provides an ideal setting for EDS measurements. While focusing on a particle for imaging purposes, the operator can simultaneously obtain an elemental map of the particle in view. This approach has been utilized in multiple studies, including observation of n-ceria and ZVI in soot aggregates,[22, 74] measuring elemental maps in diesel soot,[118] and determining the elemental content of MWCNTs in a research laboratory.[92]

Like EDS, EELS uses the electrons from the TEM or SEM beam. Instead of measuring the X-rays produced from the sample, however, EELS scatters electrons from the sample. EELS is used for quantifying and detecting elements during SEM and TEM analyses. For example, EELS has been used to observe redox changes in n-ceria upon reduction by H_2.[133]

X-Ray Diffraction (XRD) & Electron Diffraction (ED). XRD measures the diffraction of X-rays in a sample. XRD is primarily used for the detection and characterization of crystalline phases (such as soil) in a sample[54] and the differentiation of crystalline phases from amorphous phases. XRD can be especially useful for detection of soil particles or crystalline CNTs and fullerenes in the atmosphere.[42, 56] XRD has also revealed that ZVI will readily oxidize in aqueous solutions.[80]

ED is similar to XRD except electrons, instead of X-rays, are fired at the sample target. The resulting interference pattern provides an image of crystal structures in the sample. Wang et al. utilized ED to understand how n-ceria can be re-oxidized following reduction.[133] Using ED, Jung et al.[22] identified irregularities in a n-ceria crystal structure. A more thorough review of electron diffraction techniques relating to CNTs is available elsewhere.[134]

Scanning Probe Microscopy (SPM). Two common types of SPM are atomic force microscopy (AFM) and scanning tunneling microscopy (STM). In both cases, a sharp metallic tip is used to measure the force (AFM) or tunneling current (STM) between the tip and the sample. SPM techniques can sense height differences of 10 pm and can therefore create 3-D images of the sample. AFM has been used by a number of researchers to examine several different types of NPs, including CNTs, iron, and silver.[135-137] AFM has been reported to be especially useful in detecting chirality and tube length of CNTs.[138, 139]

Single-Particle Mass Spectrometry (SPMS). SPMS is a real-time mass spectrometry technique capable of determining the chemical composition of individual aerosol particles. SPMS is often used to measure C-, N-, O-, and S-containing compounds, and airborne ZVI has also been detected using this technique.[75]

Johnston et al.[140] have developed SPMS instruments specifically designed for sizing and analyzing single NPs. As with ICP-MS, SPMS techniques suffer because information regarding particle size and degree of aggregation is distorted or lost. A nanoaerosol mass spectrometer (NAMS) has also been used to measure test aerosols (e.g., NaCl, oleic acid) and to determine real-time composition of nano-aerosols in an urban area.[75, 132, 140-142] In addition, a thermal desorption chemical ionization mass spectrometer (TDCIMS) has been used to characterize 10–33 nm particles in a study in Mexico City.[143]

Field Measurements of ENPs

Field measurements are conducted to characterize ambient particles, in terms of size distribution, concentration, composition, and morphology, and are used to understand their sources and transformations. Moreover, they provide the best estimate of human and environmental exposures. Measurements of particle size distribution contribute to the understanding of particle formation and growth processes in ambient air. They are typically made along roadways or in urban centers, with simultaneous collection of samples at sites farther from the road or at rural sites, respectively, to estimate contributions of "background" sources. Additionally, they are usually designed to consider temporal, seasonal, and/or meteorological variations. In occupational settings, ENP size distributions are usually measured within the "breathing zone" of workers handling the NPs, and in additional locations, such as inside fume hoods and several meters away from the work zone. Measurements of particle composition and morphology further contribute to the understanding of particle evolution, and support identification of particle sources and potential health effects.

While research on INPs (i.e., UF particles) in the atmosphere has been ongoing for more than a decade, very few studies of atmospheric ENPs have been published. However, cerium, titanium, CNTs, fullerenes, and iron have all been identified in atmospheric UF particles. Additionally, measurements of airborne NPs in two types of NM (titania and carbon) production facilities have been reported in the literature. Existing applications of the techniques described above in atmospheric and workplace

environments, as well as corresponding investigative approaches, can be leveraged to meet the challenges of sampling and analysis of ENPs in the atmosphere. Field measurements for UF particle characterization include use of impactor samplers combined with bulk chemical analyses,[101, 103] thermal precipitators with TEM imaging,[42] and several other permutations of sampling and analysis techniques. Below we summarize available field measurements of the five types of NMs considered at the beginning of this review. Our intention is not to present an exhaustive survey of all available data, but to provide examples of measurements that illustrate important insights for differentiating ENPs from INPs in the atmosphere.

Field Measurements of NPs in the Atmosphere

Several studies have been conducted in which cerium levels were determined in various urban environments. Two studies in the Los Angeles area report average cerium concentrations of 0.19 ng m^{-3} and 1.2 ng m^{-3} in UF particles, measured with impactor- and filter-based collection methods followed by neutron activation analysis.[44, 144] Hu et al.[145] also analyzed impactor-based PM samples from several sites in the Los Angeles-Long Beach harbor, the busiest harbor in the U.S., and one urban site. They report water-soluble cerium concentrations of 0.001 to 0.003 ng m^{-3} in a $PM_{0.25}$ "quasi-ultrafine" mode measured by ICP-MS. Ntziachristos et al.[103] measured trace elements and metals in a UF mode (defined as <0.18 μm) during the winter at a location next to a busy Southern California freeway. Particles in this mode were segregated into four size fractions (180-100, 100-56, 56-32, and 32-18 nm) using a nano-MOUDI, and ICP-MS measurements showed that the percentage contribution of cerium to the total elemental mass generally decreased from largest to smallest size fraction. The authors also indicated that the percentage of cerium increased away from the freeway and that the cerium was primarily of crustal origin.

Introduction of the n-ceria-based diesel additive Envirox™ into the 7,000-vehicle fleet of Stagecoach UK Bus, one of the largest bus operators in the United Kingdom, prompted measurement of cerium in PM_{10} (diameter $\leq$ 10 μm) collected at monitoring sites at various locations in the UK. Park et

al.[93] used ICP-AES (atomic emission spectroscopy) to analyze available PM_{10} filter samples collected over approximately four-week intervals during the 12 months before and after the FBC was introduced into the bus fleet. At one site in northeast England, namely Newcastle Centre, they found a four-fold increase in the average cerium concentration from 0.145 ng m^{-3} to 0.612 ng m^{-3}. The air quality monitoring station at Newcastle Centre is located approximately 20 m from a major through road. On an average daily basis, buses on three different routes travel directly past the monitoring station 563 times, and five other routes direct buses within 100 m of the station an additional 767 times. At two sites in London, England, Park et al.[93] found no statistically significant change in the PM_{10}-cerium concentrations, as the bus fleet using the n-ceria additive represented only a small fraction of the passing traffic. While these measurements indicate an association between increased concentration of cerium in ambient particles and use of n-ceria as a FBC, they do not demonstrate whether or not the cerium is present in ambient NPs.

Studies involving titania have shown that aggregates were detected in urban UF particles.[42, 100] Sources of the n-titania are not necessarily consistent with ENPs. Therefore, it is possible that n-titania does have natural sources. Cass et al.[44] found Ti to be among the most abundant catalytic metals in UF particles collected in seven Southern California cities, with a mean concentration of 43 ng m^{-3}. Hughes et al.[144] reported an average concentration of Ti in UF particles sampled in Pasadena, CA of 7.65 ng m^{-3}. A much lower concentration (1-2 ng m^{-3}) was measured next to a busy Southern California freeway by Ntziachristos et al.[103] These values are substantially lower than concentrations measured in titania production facilities.[46, 146]

A series of articles by Murr et al. and Bang et al. focus on collection (with TP) and imaging (with TEM) of NPs in El Paso, Texas. [42, 43, 45, 63, 100, 147] During a two-year sampling study in El Paso, Texas, the authors observed aggregates ranging from two nanocrystals to thousands of nanocrystals. They note that greater than 90% of particles in the PM_1 fraction were crystalline and greater than 80% of the PM_1 fraction were aggregates of NPs. Surprisingly, 58% of the aggregates in the PM_1 fraction were less than 0.1 μm. Overall, more than 40% of the particles contained carbon, with approximately half of the carbon

in the form of CNT aggregates. Even though carbon NPs were found in each sampling trip in El Paso, number concentrations were very low compared to diesel particles and particulates from cigarette smoke. In Mexico City, fullerene-like particles were observed, while in El Paso aggregates were primarily MWCNTs ranging in size from 3 to 30 nm. [63] Additionally, Chianelli et al. observed fullerene-like materials in PM collected in Mexico City.[54] Important results have also resulted from characterization of NPs in remote environments. For example, Posfai et al. observed fullerenes over the open ocean intermixed with silicates.[148] As there are likely no natural sources of fullerenes over the open ocean, this result, along with the fact that NPs have atmospheric lifetimes ranging from months to years due to their small size, [111] has implications for long-range transport modeling of aerosols.

As the most abundant element on Earth, it is not surprising that large concentrations of iron have been measured in atmospheric NPs. Average concentrations up to 186 ng m^{-3} have been reported for UF particle samples collected in various locations in Southern California.[44, 103, 144] Concentrations of silver have also been detected in atmospheric particles: in Atlanta and in $PM_{2.5}$ in Mexico City.[149, 150] However, silver concentrations in UF atmospheric particles have not been reported.

Field Measurements of Airborne NPs in Workplaces

In two workplace studies, the highest concentration of titania measured was 7.75 mg m^{-3}.[46, 146] Particles collected inside titania production facilities were also analyzed using TEM and SEM.[89, 105] In these settings, titania aggregates were observed with sizes ranging from 0.2 to several microns, consisting of individual particles 10–80 nm in diameter.[89] This finding implies that, due to the high degree of aggregation, airborne NPs may deposit on the supermicron stages of an impactor sampler. ICP-OES was used to determine Ti concentrations, which assisted in distinguishing ENPs from INPs.[89]

Yeganeh et al.[114] sampled NPs of diameter 4-160 nm in a fullerene manufacturing facility using an SMPS with a nano-DMA. For a set of measurements conducted during one step of a production run

called sweeping, in which the raw product containing carbonaceous NMs is handled by a technician, they illustrate particle size distributions. The total number concentrations averaged 5352, 4834, and 3667 cm^{-3} in the fume hood where the NM was handled, in the work zone just outside the face of the fume hood, and in the background about 2 m away from the hood, respectively. Although concentrations of NPs with diameter less than 10 nm had large variability, they were highest inside the fume hood. Two individual measurements in the fume hood showed particle number concentrations to be significantly enhanced around 5 and 20 nm, with particles smaller than 14 nm accounting for 3-5% of those measured below 160 nm. Fujitani et al.[105] observed aggregates of carbon NPs (single particles < 100 nm) in a carbon NP production facility using TEM and SEM imaging. They collected NPs on quartz-fiber filters using an impactor sampler and also analyzed the NPs using EC-OC analysis.[105] Using this analysis technique, a distinction between INPs and ENPs became apparent. This is one of the only studies in the literature that reports a distinction of ENPs and INPs using a bulk-analysis technique.

The data summarized above demonstrates the importance of characterizing airborne NPs, whether in the atmosphere or in workplaces, to differentiate between INPs and ENPs. Simply measuring the presence of a species of interest will not be sufficient in most cases to characterize them as ENPs. The use of analytical techniques (e.g., ICP-OES and EC-OC analysis) in studies described above assisted in identifying ENPs in atmospheric samples. The limited amount of literature on field measurements of the NMs considered in this review, and lack of data on airborne n-CeO_2, ZVI NPs, and Ag NPs in workplaces, indicates a need for further research on ENPs. Additional measurements in occupational settings could provide valuable data for distinguishing ENPs from INPs in the atmosphere. Understanding ENP sources, as well as any differences between their physical and chemical characteristics and those of INPs, will be critical to evaluating their fate and transport and exposures to humans and the environment.

Conclusions

This state-of-the-science review has considered sources, characterization, transformations, sampling techniques, methods for analysis, and field measurements of selected NPs in the atmosphere. Major sources of entry into the air environment range from direct emissions of ENPs, such as n-ceria or ZVI NPs through their use as FBCs in diesel fuel, to incidental emissions of ENPs, such as n-titania, carbon NPs, and Ag NPs through wear and disposal of NM products. At the present time, the only viable means of sampling and analysis of these ENMs is by conventional methods used for UF particles. These methods have limitations in the NP regime. Despite the potential shortcomings, numerous investigators have shown that with appropriate attention to detail, filter-based and impactor samplers may be used to collect NPs for off-line characterization.

Techniques adapted for ENP measurements by various investigators were found to give reasonable results as seen from the summary of field studies. However, some compound-specific issues are present for the selected NPs. For cerium and titanium, specific identification techniques, such as ICP, can be limited by the presence of high background concentrations from natural sources. Other issues can arise. For example, identification from only bulk analysis samples can be made for cerium emitted as n-ceria in FBC applications. While measurements in workplaces have the advantage of high concentrations of ENPs relative to INPs, such studies may be drawn upon to inform sampling and analysis methods used for atmospheric aerosols, as well as distinction between INPs and ENPs. A review of ENP measurements in workplaces was beyond the scope of this work, but can be found elsewhere.[151, 152] Considerable methods development is needed to identify the selected NPs in specific size fractions of ambient aerosols.

Disclaimer

The authors wish to thank Prof. Linsey Marr of Virginia Technical Institute, Dr. Nancy Jennerjohn of the University of California, Los Angeles, Environmental Health Sciences Department for discussion of analytical issues related to the measurements of ENPs, and Prof. Constantinos Sioutas of the

University of Southern California for providing ambient measurement data. The authors also wish to acknowledge Michele Conlon (U.S. EPA), Pramod Kulkarni (CDC-NIOSH), Sotiris Pratsinis (ETH Zurich), and Walter Copan (formerly of CDT, Inc.). The U.S. Environmental Protection Agency through its Office of Research and Development funded and collaborated in the research described here under Contract EP-D-05-065 to Alion Science and Technology. The manuscript is subjected to external peer review and has been cleared for publication. Mention of trade names or commercial products does not constitute an endorsement or recommendation for use.

References

1. Oberdorster G, Oberdorster, E. Oberdorster J. Nanotoxicology: an emerging discipline evolving from studies of ultrafine particles. Environ Health Perspec. 2005; 113(7): 823.
2. Hood E. Nanotechnology: Looking as we leap. Environ Health Perspec. 2004; 112(13): A740-A749.
3. Tsuji, JS, Maynard AD, Howard PC, James JT, Lam C, Warheit DB, Santamaria AB. Research strategies for safety evaluation of nanomaterials, part IV: Risk assessment of nanoparticles. Toxicol Sci. 2006; 89(1): 42-50.
4. Stone V, Johnston H, Clift MJD. Air pollution, ultrafine and nanoparticle toxicology: Cellular and molecular interactions. IEEE Trans Nanobioscience. 2007: 6(4): 331-340.
5. Meyer DE, Curran MA, Gonzalez MA. An Examination of Existing Data for the Industrial Manufacture and Use of Nanocomponents and their Role in the Life Cycle Impact of Nanoproducts. Environ Sci Technol. 2009; 43(5): 1256-1263.
6. Englert BC. Nanomaterials and the environment: uses, methods and measurement. J Environ Monitor. 2007; 9(11): 1154-1161.
7. Cass, GR, Hughes LA, Bhave P, Kleeman MJ, Allen JO, Salmon LG. The chemical composition of atmospheric ultrafine particles. Phil Trans Royal Soc A, 2000; 358(1775) 2581-2592.
8. Niessner R. Chemical Characterization of Aerosols - online and in situ. Angew Chem – (International Edition in English). 1991; 30(5): 466-476.
9. Auffan M, Rose J, Wiesner MR, Bottero J-Y. Chemical stability of metallic nanoparticles: A parameter controlling their potential cellular toxicity in vitro. Environ. Poll. 2009; 157(4): 1127-1133.
10. Adamson IYR, Prieditis H, Vincent R. Pulmonary toxicity of an atmospheric particulate sample is due to the soluble fraction. Toxicol Appl Pharmacol. 1999; 157(1): 43-50.
11. Camner P, Johansson A. Reaction of Alveolar Macrophages To Inhaled Metal Aerosols. Environ Health Perspec. 1992; 97: 185-188. Dreher KL. Health and environmental impact of nanotechnology: Toxicological assessment of manufactured nanoparticles. Toxicol Sci. 2004; 77(1): 3-5.

12. von Klot S, Wölke G, Tuch T, Heinrich J, Dockery DW, Schwartz J, Kreyling WG, Wichmann HE, Peters A. Increased asthma medication use in association with ambient fine and ultrafine particles. Eur Respir J. 2002; 20(3): 691-702.

13. Nowack B, Bucheli TD. Occurrence, behavior and effects of nanoparticles in the environment. Environ Pollut. 2007; 150(1): 5-22.

14. Kittelson DB. Engines and nanoparticles: A review. J Aerosol Sci. 1998; 29(5-6): 575-588.

15. U.S. Environmental Protection Agency, Nanotechnology White Paper. 2007; U.S. EPA: Washington, DC, EPA100/B-07/001; U.S. Environmental Protection Agency, Nanomaterials Research Strategy, 2009; U.S. EPA: Washington DC, EPA 620/K-09/011; (www.epa.gov/nanoscience/).

16. Hedrick JB. Rare Earths, in Minerals Yearbook Vol I: Metals and Minerals. 1998, USGS: Reston, VA. p. 61.1-61.14.

17. Reff A, Bhave PV, Simon H, Pace TG, Pouliot GA, Mobley JD, Houyoux M. Emissions Inventory of $PM_{2.5}$ Trace Elements across the United States. Environ Sci Technol, 2009. 43(15) 5790-5796.

18. Reinhardt K, Winkler H. (1996) Cerium mischmetal, cerium alloys, and cerium compounds. In: Ullmann's encyclopedia of industrial chemistry. Vol. A6. Weinheim, Germany: Wiley-VCH; p. 139-152.

19. Costatini M. Evaluation of Human Health Risk from Cerium Added to Diesel Fuel. 2001; Health Effects Institute.

20. Corma A, Atienzar P, García H, Chane-Ching J-Y. Hierarchically mesostructured doped CeO_2 with potential for solar-cell use. Nature Materials. 2004; 3(6): 394-397.

21. Pati RK, Lee IC, Chu DR, Hou SC, Ehrman S.H. Nanosized ceria-based water-gas shift (WGS) catalyst for fuel cell applications. Abstracts of the American Chemical Society, 2004; 228: 220-FUEL.

22. Jung HJ, Kittelson DB, Zachariah MR. The influence of a cerium additive on ultrafine diesel particle emissions and kinetics of oxidation. Combustion and Flame, 2005; 142(3): 276-288

23. Cerulean International Limited, 211b Submission Tier 1 Summary Report for Envirox™, non-confidential version, 2005.

24. Copan, W., *Personal Communication*, 2009.

25. Karakoti AS, Monteiro-Riviere NA, Aggarwal R, Davis JP, Narayan RJ, Self WT, McGinnis J, Seal S. Nanoceria as antioxidant: Synthesis and biomedical applications. J Miner Metal Material Soc. 2008; 60(3): 33-37.

26. Machida M, Murata Y, Kishikawa K, Zhang D, Ikeue K. On the reasons for high activity of CeO_2 catalyst for soot oxidation. Chemistry of Materials. 2008; 20(13): 4489-4494.

27. Ntainjua E, Taylor SH. The catalytic total oxidation of polycyclic aromatic hydrocarbons. Topics in Catalysis. 2009; 52(5): 528-541.

28. Simonsen SB, Dahl S, Johnson E, Helveg S. Ceria-catalyzed soot oxidation studied by environmental transmission electron microscopy. J Catalysis. 2008; 255(1): 1-5.

29. Lahaye J, Boehm S, Chambrion Ph., Ehrburger P. Influence of cerium oxide on the formation and oxidation of soot. Combustion and Flame. 1996; 104(1-2): 199-207.

30. Summers JC, Van Houtte S, Psaras D. Simultaneous control of particulate and NO_x emissions from diesel engines. Appl Cataly B: Environmental, 1996. 10: 139-156.

31. Okuda T, Schauer JJ, Olson MR, Shafer MM, Rutter AP, Walz KA, Morshauser PA. Effects of a platinum-cerium bimetallic fuel additive on the chemical composition of diesel engine exhause particles. Energy & Fuels. 2009; 23: 4874-4980.

32. Skillas G, Qian Z, Baltensperger U, Matter U, Burtscher H. The influence of additives on the size distribution and composition of particles produced by diesel engines. Combust Sci Technol. 2000; 154: 259-273.

33. Heckert EG, Karakoti AS, Seal S, Self WT. The role of cerium redox state in the SOD mimetic activity of nanocerium. Biomaterials. 2008; 29: 2705-2709.

34. Cervini-Silva J, Fowle D, Banfield JF. Biogenic dissolution of soil cerium-phosphate minerals. Am. J. Sci. 2005; 305: 711-726.

35. Kiser MA, Westerhoff P, Benn T, Wang T, Pérez-Rivera J, Hristovski K. Titanium Nanomaterial removal and release from wastewater treatment plants. Environ Sci Technol. 2009. 43, 6757-6763.

36. Klaine SJ, Pedro, Alvarez JJ, Batley GE, Fernandes TF, Handy RD, Lyon DY, Mahendra S, McLaughlin MJ, Lead JR. Nanomaterials in the environment: Behavior, fate, bioavailability, and effects. Environ Toxicol Chem. 2008; 27(9): 1825-1851.

37. Daniels SL. On the qualities of the air as affected by radiant energies (photocatalytic ionization processes for remediation of indoor environments). J Environ Engineer Sci. 2007; 6(3): 329-342.

38. Besov AS, Krivova NA, Vorontsov AV, Zaeva OB, Kozlov DV, Vorozhtsov AB, Parmon VN, Sakovich GV, Komarov VF, Smirniotis PG, Eisenreich N. Air detoxification with nanosize TiO_2 aerosol tested on mice. J Hazard Mater. 2010; 173: 40-46.

39. Han F, Kambala VSR, Srinivasan M, Rajarathnam D, Naidu R. Tailored titanium dioxide photocatalysts for the degradation of organic dyes in wastewater treatment: A review. Appl Catal A: Gen. 2009. **359**: p. 25-40.

40. Yang Z-P, Zhang, C-J. Mechanism and kinetics of Pb(II) adsorption on ultrathin nanocrystalline titania coatings removal of lead from wastewater. J Hazard Mater. 2009; 172: 1082-1086.

41. Narr J, Viraraghavan T, Jin Y-C. Applications of nanotechnology in water/wastewater treatment: A Review. Fresnius Environ Bull. 2007; 16(4): 320-329.

42. Bang JJ, Murr LE, Esquivel EV. Collection and characterization of airborne nanoparticulates. Materials Characteriz. 2004; 52(1): 1-14.

43. Murr LE, Esquivel EV, Bang JJ. Characterization of nanostructure phenomena in airborne particulate aggregates and their potential for respiratory health effects. J Materials Sci-Materials in Medicine. 2004; 15(3): 237-247.

44. Cass, GR, Hughes LA, Bhave P, Kleeman MJ, Allen JO, Salmon LG. The chemical composition of atmospheric ultrafine particles. Phil Trans Royal Soc A. 2000; 358(1775) 2581-2592.

45. Murr LE, Soto KF, Garza KM, Guerrero PA, Martinez F, Esquivel EV, Ramirez DA, Shi Y, Bang JJ, Venzor J. Combustion-generated nanoparticulates in the El Paso, TX, USA / Juarez, Mexico Metroplex: their comparative characterization and potential for adverse health effects. Inter J Environ Res Pub Health 2006; 3: 48-66.

46. Berges M, Mohlmann B, Swennen YV, Rompaey P, Berghmans P. Workplace exposure characterization TiO_2 nanoparticle production. In Proceedings of the 3rd International Symposium in Nanotechnology, Occupational and Environmental Health. 2007; Taipei, Taiwan.

47. Chen LX, Rajh T, Wang Z, Thurnauer MC. XAFS studies of surface structures of TiO_2 nanoparticles and photocatalytic reduction of metal ions. J Phys Chem B. 1997; 101(50): 10688-10697.

48. Jang, HD, Kim SK, Kim SJ. Effect of particle size and phase composition of titanium dioxide nanoparticles on the photocatalytic properties. J Nanopart Res. 2001; 3(2-3): 141-147.

49. Jung KY, Park SB. Anatase-phase titania - preparation by embedding silica and photocatalytic activity for the decomposition of trichloroethylene. J Photochem Photobiol A – Chem. 1999; 127: 117.

50. Fox MA, Dulay MT. Heterogeneous Photocatalysis. Chem Rev. 1993; 93(1): 341-357.

51. Liqiang J, Baifu X, Fulong Y, Baiqi W, Keying S, Weimin C, Honggang F. Deactivation and regeneration of ZnO and TiO_2 nanoparticles in the gas phase photocatalytic oxidation of n-C_7H_{16} or SO_2. Appl Cataly A-Gen. 2004; 275(1-2): 49-54.

52. Egerton TA, Mattinson JA. Comparison of photooxidation and photoreduction reactions on TiO_2 nanoparticles. J Photochem Photobiol A-Chem. 2007; 186(2-3): 115-120.

53. Williams DS, Shukla MK, Ross J. Particulate matter emission by a vehicle running on unpaved road. Atmos Environ. 2008; 42(16): 3899-3905.

54. Chianelli RR, Yácaman MJ, Arenas J, Aldape F. Atmospheric nanoparticles in photocatalytic and thermal production of atmospheric pollutants. J Hazard Sub Res - Vol 1. 1998; p. 1-1.

55. Murr LE, Bang JJ, Lopez DA, Guerrero PA, Esquivel EV, Choudhuri AR, Subramanya M, Morandi M, Holian A. Carbon nanotubes and nanocrystals in methane combustion and the environmental implications. J Materials Sci. 2004; 39(6): 2199-2204.

56. Bang JJ, Guerrero PA, Lopez DA, Murr LE, Esquivel EV. Carbon nanotubes and other fullerene nanocrystals in domestic propane and natural gas combustion streams. J Nanosci Nanotechnol. 2004; 4(7): 716-718.

57. Helland A, Scheringer M, Siegrist M, Kastenholz HG, Wiek A, Scholz RW. Risk assessment of engineered nanomaterials: A survey of industrial approaches. Environ Sci Technol. 2008; 42(2): 640-646.

58. Langa F, Nierengarten J-F, Eds. Fullerenes: principles and applications. Royal Society of Chemistry, Cambridge, UK, 2007.

59. Quadros ME, Marr LC. Environmental and human health risks of airborne silver nanoparticles. J Air Waste Manage Assoc. (in press).

60. Wick P, Manser P, Limbach LK, Dettlaff-Weglikowska U, Krumeich F, Roth S, Stark WJ, Bruinink A. The degree and kind of agglomeration affect carbon nanotube cytotoxicity. Toxicol Lett. 2007; 168(2): 121-131.

61. Krusic PJ, Wasserman E, Keizer PN, Morton JR, Preston KF. Radical reactions of C_{60}. Science. 1991; 254: 1183-1185.

62. Markus A, Nairz O, Voss-Andreae J, Keller C, van der Zouw G, Zeilinger A. Wave-particle duality of C_{60}. Nature. 1999; 401: 680-682.

63. Murr LE, Bang JJ, Esquivel EV, Guerrero PA, Lopez A. Carbon nanotubes, nanocrystal forms, and complex nanoparticle aggregates in common fuel-gas combustion sources and the ambient air. J Nanopart Res. 2004; 6(2-3): 241-251.

64. Donaldson K, Aitken R, Tran L, Stone V, Duffin R, Forrest G, Alexander A. Carbon nanotubes: A review of their properties in relation to pulmonary toxicology and workplace safety. Toxicol Sci. 2006; 92(1): 5-22.

65. Xu YJ, Li J.Q. The interaction of N-2 with active sites of a single-wall carbon nanotube. Chem Phys Lett. 2005; 412(4-6): 439-443.

66. Ulbricht H, Moos G, Hertel T. Interaction of molecular oxygen with single-wall carbon nanotube bundles and graphite. Surface Sci. 2003; 532: 852-856.

67. Goldoni A, Larciprete R, Petaccia L, Lizzit S. Single-wall carbon nanotube interaction with gases: Sample contaminants and environmental monitoring. J Amer Chem Soc. 2003; 125(37): 11329-11333.

68. Chibante LPF, Heymann D. On the geochemistry of fullerenes - stability of C60 in ambient air and the role of ozone. Geochimica Et Cosmochimica Acta. 1993; 57: 1879-1881.

69. Scanlon JC, Brown JM, Ebert LB. Oxidative Stability of Fullerenes. J Phys Chem. 1994; 98: 3921-3923.

70. Cataldo, F. Ozone reaction with carbon nanostructures 1: Reaction between solid C-60 and C-70 fullerenes and ozone. J Nanosci Nanotechnol. 2007; 7: 1439-1445.

71. Watanabe H, Matsui E, Ishiyama Y, Senna M. Solvent free mechanochemical oxygenation of fullerene under oxygen atmosphere. Tetrahed Lett. 2007; 48: 8132-8137.

72. Theron J, Walker JA, Cloete TE. Nanotechnology and Water Treatment: Applications and Emerging Opportunities. Criti Rev Microbiol. 2008; 34: 43-69.

73. Health Canada. A review of chemical additives present in diesel fuels used in Canada and the United States of America. 2006; Ottawa, Ontario, Canada.

74. Miller A, Ahlstrand G, Kittelson D, Zachariah M. The fate of metal (Fe) during diesel combustion: Morphology, chemistry, and formation pathways of nanoparticles. Combustion and Flame, 2007; 149(1-2): 129-143.

75. Lee D, Miller A, Kittelson D, Zachariah MR. Characterization of metal-bearing diesel nanoparticles using single-particle mass spectrometry. J Aero Sci. 2006; 37(1): 88-110.

76. Zhang J, Megaridis CM. Soot suppression by ferrocene in laminar ethylene/air nonpremixed flames. Combustion and Flame. 1996; 105(4): 528-540.

77. Maynard AD, Ku BK, Emery M, Stolzenburg M, McMurry PH. Measuring particle size-dependent physicochemical structure in airborne single walled carbon nanotube agglomerates. J Nanopart Res. 2007; 9(1): 85-92.

78. Keenan CR, Goth-Goldstein R, Lucas D, Sedlak DL. Oxidative Stress Induced by Zero-Valent Iron Nanoparticles and Fe(II) in Human Bronchial Epithelial Cells. Environ Sci Technol. 2009; 43(12): 4555-4560.

79. Keenan CR, Sedlak DL. Ligand-enhanced reactive oxidant generation by nanoparticulate zero-valent iron and oxygen. Environ Sci Technol. 2008; 42(18): 6936-6941.

80. Auffan M, Achouak W, Rose J, Roncato M-A, Chaneac C, Waite DT, Masion A, Woicik JC, Wiesner WR, Bottero JY. Relation between the redox state of iron-based nanoparticles and their cytotoxicity toward Escherichia coli. Environ Sci Technol. 2008; 42(17): 6730-6735.

81. Tolaymat TM, El Badawy AM, Genaidy A, Scheckel KG, Luxton TP, Suidan M. An evidence-based environmental perspective of manufactured silver nanoparticle in syntheses and applications: A systematic review and critical appraisal of peer-reviewed scientific papers. Sci Total Environ. 2010; 408: 999-1006.

82. Luoma S N. Silver nanotechnologies and the environment: Old problems or new challenges? Woodrow Wilson International Center for Scholars, September 2008: p. 558.

83. El Badawy AM, Luxton TP, Silva RG, Scheckel KG, Suidan MT, Tolaymat TM. Impact of environmental conditions (pH, ionic strength, and electrolyte type) on the surface charge and aggregation of silver nanoparticles suspensions. Environ Sci Technol. 2010; 44(4): 1260-1266.

84. Shin, WG, Wang J, Mertler M, Sachweh B, Fissan H, Pui DYH. Structural properties of silver nanoparticle agglomerates based on transmission electron microscopy: relationship to particle mobility analysis. J Nanopart Res. 2009; 11(1): 163-173.

85. McMahon MD, Lopez R, Meyer III HM, Feldman LC, Haglund Jr RF. Rapid tarnishing of silver nanoparticles in ambient laboratory air. Appl Phys B: Lasers and Optics. 2005; 80(7): 915-921.

86. Tobias HJ, Beving DE, Ziemann PJ, Sakurai H, Zuk M, McMurry PH, Zarling D, Waytulonis R, Kittelson DB. Chemical analysis of diesel engine nanoparticles using a nano-DMA/thermal desorption particle beam mass spectrometer. Environ Sci Technol. 2001; 35(11): 2233-2243.

87. Shi JP, Harrison RM. Investigation of ultrafine particle formation during diesel exhaust dilution. Environ Sci Technol. 1999; 33(21): 3730-3736.

88. Shi JP, Mark D, Harrison RM. Characterization of particles from a current technology heavy-duty diesel engine. Environ Sci Technol. 2000; 34(5): 748-755.

89. Peters TM, Elzey S, Johnson R, Park H, Grassian VH, Maher T,O'Shaughnessy PT. Airborne Monitoring to Distinguish Engineered Nanomaterials from Incidental Particles for Environmental Health and Safety. J Occup Environ Hyg. 2009; 6(2): 73-81.

90. Burdett GJ, Rood AP. Membrane-filter, direct-transfer technique for the analysis of asbestos fibers or other inorganic particles by transmission electron microscopy. Environ Sci Technol. 1983; 17(11): 643-648.

91. Burdett GJ, Rood AP. Sample preparation for monitoring asbestos in air by transmission electron microscopy. Anal Chem. 1983; 55(9): 1642-1645.

92. Han JH, Lee EJ, Lee JH, So KP, Lee YH, Bae GN, Lee S-B, Ji JH, Cho MH, Yu IJ. Monitoring multiwalled carbon nanotube exposure in carbon nanotube research facility. Inhal Toxicol. 2008; 20(8): 741-749.

93. Park B, Donaldson K, Duffin R, Tran L, Kelly F, Mudway I, Morin J-P, Guest R, Jenkinson P, Samaras Z, Giannouli M, Kouridis H, Martin P, Hazard and risk assessment of a nanoparticulate cerium oxide-based diesel fuel additive – A case study. Inhal Toxicol. 2008; 20(6): 547-566.

94. Jang J, Akin D, Lim KS, Broyles S, Ladisch MR, Bashir R. Capture of airborne nanoparticles in swirling flows using non-uniform electrostatic fields for bio-sensor applications. Sensors and Actuators B-Chem. 2007; 121(2): 560-566.

95. Dahl A, Gharibi A, Swietlicki E, Gudmundsson A, Bohgard M, Ljungman A, Blomqvist G, Gustafsson M. Traffic-generated emissions of ultrafine particles from pavement-tire interface. Atmos Environ. 2006; 40(7): 1314-1323.

96. Ku BK, Maynard AD. Generation and investigation of airborne silver nanoparticles with specific size and morphology by homogeneous nucleation, coagulation and sintering. J Aero Sci. 2006; 37(4): 452-470.

97. Siegmann K, Scherrer L, Siegmann HC. Physical and chemical properties of airborne nanoscale particles and how to measure the impact on human health. J Molec Struct-Theochem. 1999; 458(1-2): 191-201.

98. Qian ZQ, Siegmann K, Keller A, Matter U, Scherrer L, Siegmann HC. Nanoparticle air pollution in major cities and its origin. Atmos Environ. 2000; 34(3): 443-451.

99. Murr LE, Soto KF. A TEM study of soot, carbon nanotubes, and related fullerene nanopolyhedra in common fuel-gas combustion sources. Materials Characterization. 2005; 55(1): 50-65.

100. Murr LE, Soto KF, Esquivel EV, Bang JJ, Guerrero PA, Lopez DA, Ramirez DA. Carbon nanotubes and other fullerene-related nanocrystals in the environment: A TEM study. J Material Sci. 2004; 56(6): 28-31.

101. Fang GC, Wu YS, Wen CC, Lin CK, Huang SH, Rau JY, Lin CP. Concentrations of nano and related ambient air pollutants at a traffic sampling site. Toxicol Ind Health. 2005; 21(10): 259-271.

102. Grose M, Sakurai H, Savstrom J, Stolzenburg MR, Watts WF, Morgan CG, Murray IP, Twigg MV, Kittelson DB, McMurry PH. Chemical and physical properties of ultrafine diesel exhaust particles sampled downstream of a catalytic trap. Environ Sci Technol. 2006; 40(17): 5502-5507.

103. Ntziachristos L, Ning Z, Geller MD, Sheesley RJ, Schauer JJ, Sioutas C. Fine, ultrafine and nanoparticle trace element compositions near a major freeway with a high heavy-duty diesel fraction. Atmos Environ, 2007; 41(27): 5684-5696.

104. Fushimi A, Hasegawa S, Takahashi K, Fujitani Y, Tanabe K, Kobayashi S. Atmospheric fate of nuclei-mode particles estimated from the number concentrations and chemical composition of particles measured at roadside and background sites. Atmos Environ. 2008; 42(5): 949-959.

105. Fujitani Y, Kobayashi T. Measurement of Aerosols In Engineered Nanomaterials Factories For Risk Assessment. Nano. 2008; 3(4): 245-249.

106. TSI, *TSI Incorporated - Models - 3080 series*. 2009.

107. Jennerjohn, N., *Personal Communication*, 2009.

108. Cheng YS, Yeh, HC. Analysis of screen diffusion battery data. *Am. Ind. Hyg. Assoc. J.* 1984; 45: 556-561.

109. Cheng YS, Yeh HC, Newton GJ. Sampling in Tandem With Other Instruments. In *Cascade Impactor: Sampling and Analysis* (J.P. Lodge, Jr.; T.L. Chan, eds). 1986; American Industrial Hygiene Association, Akron, OH, p. 129.

110. Barr EB, Cheng YS, Yeh HC, Wolff RK. Size characterization of carbonaceous particles using a Lovelace Multijet Cascade Impactor/Parallel-Flow Diffusion Battery serial sampling train. Aero Sci Technol. 1989; 10: 1205-1212.

111. Shi JP, Evans DE, Khan AA, Harrison RM. Sources and concentration of nanoparticles (< 10 nm diameter) in the urban atmosphere. Atmos Environ. 2001; 35(7): 1193-1202.

112. Minoura H, Takekawa H. Observation of number concentrations of atmospheric aerosols and analysis of nanoparticle behavior at an urban background area in Japan. Atmos Environ. 2005; 39(32): 5806-5816.

113. Watson JG, Chow JC, Lowenthal DH, Kreisberg NM, Hering SV, Stolzenburg MR. Variations of nanoparticle concentrations at the Fresno Supersite. Sci Total Environ. 2006; 358(1-3): 178-187.

114. Yeganeh B, Kull CM, Hull MS, Marr LC. Characterization of airborne particles during production of carbonaceous nanomaterials. Environ Sci Technol. 2008; 42(12): 4600-4606.

115. Jacobson MZ, Kittelson DB, Watts WF. Enhanced coagulation due to evaporation and its effect on nanoparticle evolution. Environ Sci Technol. 2005; 39(24): 9486-9492.

116. Charron A, Harrison RM. Primary particle formation from vehicle emissions during exhaust dilution in the roadside atmosphere. Atmos Environ. 2003; 37(29): 4109-4119.

117. Gramotnev DK, Gramotnev G. A new mechanism of aerosol evolution near a busy road: fragmentation of nanoparticles. J Aero Sci. 2005; 36(3): 323-340.

118. Mathis U, Kaegi R, Mohr M, Zenobi R. TEM analysis of volatile nanoparticles from particle trap equipped diesel and direct-injection spark-ignition vehicles. Atmos Environ. 2004; 38(26): 4347-4355.

119. Watson JG, Chow JC, Park K, Lowenthal DH. Nanoparticle and ultrafine particle events at the Fresno Supersite. J Air Waste Manage Assoc. 2006; 56(4): 417-430.

120. Higgins KJ, Jung H, Kittelson DR, Roberts JT, Zachariah MR. Kinetics of diesel nanoparticle oxidation. Environ Sci Technol. 2003; 37(9): 1949-1954.

121. Zhao B, Yang Z, Wang J, Johnston MV, Wang H. Analysis of soot nanoparticles in a laminar premixed ethylene flame by scanning mobility particle sizer. Aero Sci Technol. 2003; 37(8): 611-620.

122. Tsai S-J, Hofmann M, Hallock M, Ada E, Kong J, Ellenbecker M. Characterization and evaluation of nanoparticle release during the synthesis of single-walled and multiwalled carbon nanotubes by chemical vapor deposition. Environ Sci Technol. 2009; 43: 6017-6023.

123. Lam CW, James JT, McCluskey R, Hunter RL. Pulmonary toxicity of single-wall carbon nanotubes in mice 7 and 90 days after intratracheal instillation. Toxicol Sci. 2004; 77(1): 126-134.

124. Chow JC, Watson JG, Crow D, Lowenthal DH, Merrifield T. Comparison of IMPROVE and NIOSH carbon measurements. Aero Sci Technol. 2001; 34(1): 23-34.

125. Okazaki T, Saito T, Matsuura K, Ohshima S, Yumura M, Iijima S. Photoluminescence mapping of "as-grown" single-walled carbon nanotubes: A comparison with micelle-encapsulated nanotube solutions. Nano Lett. 2005; 5(12): 2618-2623.

126. Okazaki T, Saito T, Matsuura K, Ohshima S, Yumura M, Oyama Y, Saito R, Iijima S. Photoluminescence and population analysis of single-walled carbon nanotubes produced by CVD and pulsed-laser vaporization methods. Chem Phys Lett. 2006; 420(4-6): 286-290.

127. Jones M, Engtrakul C, Metzger WK, Ellingson RJ, Nozik AJ, Heben MJ, Rumbles G. Analysis of photoluminescence from solubilized single-walled carbon nanotubes. Phys Rev B. 2005; 71(11): 10.1103/PhysRevB.71.115426.

128. Jones M, Metzger WK, McDonald TJ, Engtrakul C, Ellingson RJ, Rumbles G, Heben MJ. Extrinsic and intrinsic effects on the excited-state kinetics of single-walled carbon nanotubes. Nano Lett. 2007; 7(2): 300-306.

129. Tantra R, Cumpson P. The detection of airborne carbon nanotubes in relation to toxicology and workplace safety. Nanotoxicol. 2007; 1(4): 251-265.

130. Majestic BJ, Shafer M.M. EXAFS spectroscopy of platinum in diesel exhaust particles. Unpublished data, 2006.

131. Spence JCH. High-resolution electron microscopy. 3rd ed. Monographs on the Physics and Chemistry of Materials. 2003; USA: Oxford University Press.

132. Wang SY, Zordan CA, Johnston MV. Chemical characterization of individual, airborne sub-10-nm particles and molecules. Anal Chem. 2006; 78(6): 1750-1754.

133. Wang R, Crozier PA, Sharma R. Structural Transformation in Ceria Nanoparticles during Redox Processes. J Phys Chem C. 2009; 113(14): 5700-5704.

134. Amelinckx S, Lucas A, Lambin P. Electron diffraction and microscopy of nanotubes. Reports on Progress in Physics. 1999; 62(11): 1471-1524.

135. Biro LP, Gyulai J, Lambin P, Nagy JB, Lazarescu S, Mark GI, Fonseca A, Surján PR, Szekeres Z, Thiry PA, Lucas AA. Scanning tunneling microscopy (STM) imaging of carbon nanotubes. Carbon. 1998; 36(5-6): 689-696.

136. Tsang SC, de Oliveira P, Davis JJ, Green MLH, Hill HAO. The structure of the carbon nanotube and its surface topography probed by transmission electron microscopy and atomic force microscopy. Chem Phys Lett. 1996; 249(5-6): 413-422.

137. Zhang Y, Yang M, Ozkan M, Ozkan CS. Magnetic force microscopy of iron oxide nanoparticles and their cellular uptake. Biotechnol Progr. 2009; 25(4): 923-928.

138. Volodin A, Ahlskog M, Seynaeve E, Van Haesendonck C, Fonseca A, Nagy JB. Imaging the elastic properties of coiled carbon nanotubes with atomic force microscopy. Phys Rev Lett. 2000; 84(15): 3342-3345.

139. Singjai P, Songmee N, Tunkasiri T, Vilaithong T. Atomic force microscopy imaging and cutting of beaded carbon nanotubes deposited on glass. Surface Interface Anal. 2002; 33(10-11): 900-904.

140. Johnston MV, Wang SY, Reinard MS. Nanoparticle mass spectrometry: Pushing the limit of single particle analysis. Appl Spectrosc. 2006; 60(10): 264A-272A.

141. Zordan CA, Wang S, Johnston MV. Time-resolved chemical composition of individual nanoparticles in urban air. Environ Sci Technol. 2008; 42(17): 6631-6636.

142. Wang SY, Johnston MV. Airborne nanoparticle characterization with a digital ion trap-reflection time of flight mass spectrometer. Intern J Mass Spect. 2006; 258(1-3): 50-57.

143. Smith JN, Dunn MJ, VanReken TM, Iida K, Stolzenburg MR, McMurry PH, Huey LR. Chemical composition of atmospheric nanoparticles formed from nucleation in Tecamac, Mexico: Evidence for an important role for organic species in nanoparticle growth. Geophys Res Lett. 2008; 35: L04808.

144. Hughes LS, Cass GR, Gone J, Ames M, Olmez I. Physical and chemical characterization of atmospheric ultrafine particles in the Los Angeles area. Environ Sci Technol. 1998; 32(9): 1153-1161.

145. Hu S, Polidori A, Arhami M, Shafer MM, Schauer JJ, Cho A, Sioutas C. Redox activity and chemical speciation of size fractioned PM in the communities of the Los Angeles-Long Beach Harbor. Atmos Chem Phys. 2008; 8(21): 6439-6451.

146. Fryzek JP, Chadda B, Marano D, White K, Schweitzer S, McLaughlin JK, Blot, WJ. A cohort mortality study among titanium dioxide manufacturing workers in the United States. J Occup Environ Med. 2003; 45(4): 400-409.

147. Murr LE, Bang JJ. Electron microscope comparisons of fine and ultra-fine carbonaceous and non-carbonaceous, airborne particulates. Atmos Environ. 2003; 37(34): 4795-4806.

148. Posfai M, Anderson JR, Buseck PR, Sievering H. Soot and sulfate aerosol particles in the remote marine troposphere. J Geophys Res-Atmos. 1999; 104(D17): 21685-21693.

149. Chow JC, Watson JG, Edgerton SA, Vega E. Chemical composition of $PM_{2.5}$ and PM_{10} in Mexico City during Winter 1997. Sci Total Environ. 2002; 287(3): 177-201.

150. Lee S-H, Murphy DM, Thomson DS, Middlebrook AM. Chemical components of single particles measured with particle analysis by laser mass spectrometry (Palms) during the Atlanta Supersite Project: Focus on organic/sulfate, lead, soot, and mineral particles. J Geophys Res. 2002; 107(D1-D2): 4003. doi:10.1029/2000jd000011.

151. Maynard AD, Kuempel ED. Airborne nanostructured particles and occupational health. J of Nanopart Res. 2005; 7(6): 587-614.

152. Ono-Ogasawara M, Serita F, Takaya M. Distinguishing nanomaterial particles from background airborne particulate matter for quantitative exposure assessment. J Nanopart Res. 2009; 11(7): 1651-1659.

Appendix

Acronym Definitions

AAS	atomic absorption spectroscopy
AFM	atomic force microscopy
Ag NP	silver nanoparticle
CNT	carbon nanotube
DC	diffusion charging
DMA	differential mobility analyzer
DPM	diesel particulate matter
EC	elemental carbon
ED	electron diffraction
EDS	energy-dispersive spectroscopy
EDX	energy-dispersive X-ray spectroscopy
EEPS	Engine Exhaust Particle Sizer
EELS	electron energy loss spectroscopy
ENM	engineered nanomaterial
ENP	engineered nanoparticle
ETEM	environmental transmission electron microscopy
EXAFS	extended X-ray absorption fine structure
FAAS	flame atomic absorption spectroscopy
FBC	fuel-borne catalyst
FMPS	fast mobility particle analyzer
GC-MS	gas chromatography–mass spectrometry
ICP-AES	inductively coupled plasma–atomic emission spectroscopy
ICP-MS	inductively coupled plasma–mass spectrometry
ICP-OES	inductively coupled plasma–optical emission spectroscopy
IMPROVE	Interagency Monitoring of Protected Visual Environments
INP	incidental nanoparticle
LPI	low-pressure impactor
LVI	low-volume impactor
MCE	mixed-cellulose ester
MOUDI	Micro-Orifice Uniform-Deposit Impactor
MWCNT	multi-wall carbon nanotube
NAMS	nanoaerosol mass spectrometer
NIOSH	National Institute for Occupational Safety and Health
NM	nanomaterial
NP	nanoparticle
NT	nanotube
(p)PAH	(particulate) polycyclic aromatic hydrocarbon
PC	photoelectric charging
PCIS	personal cascade impactor sampler
PFDB	parallel flow diffusion battery
PM	particulate matter
ROS	reactive oxygen species
SEM	scanning electron microscopy
SERS	surface enhanced Raman spectroscopy
SMPS	Scanning Mobility Particle Sizer
SPM	scanning probe microscopy

SPMS	single-particle mass spectrometry
STM	scanning tunneling microscopy
STN (CSN)	Speciation Trends Network (now called: Chemical Speciation Network)
SWCNT	single-wall carbon nanotube
TDCIMS	thermal desorption chemical ionization mass spectrometry
TEM	transmission electron microscopy
TSCA	Toxic Substance Control Act
TP	thermophoretic precipitator
UF	ultrafine
VOC	volatile organic compound
XANES	X-ray absorption near-edge structure
XAS	X-ray absorption spectroscopy
XRD	X-ray diffraction
XRF	X-ray fluorescence spectroscopy
ZVI NP	zero valent iron nanoparticle

List of Figures

List of Tables

Table 1. Nanomaterials considered in the U.S. EPA Office of Research and Development Nanomaterial Research Strategy.

Nanomaterial	Chemical Form(s)	Significant Uses	Selected Physical/ Chemical Characteristics	Atmospheric transformations (itself and other pollutants)	References
n-Ceria (n-Ce)	n-CeO_2; $Ce(OH)_2$	Fuel-borne catalyst to control diesel emissions	n-CeO_2 strong soot oxidizer; 5-7 nm primary particles	n-Ce fate unknown	16-21; 25-31
n-Titania (n-Ti)	n-TiO_2	Additive to paints, cosmetics; photocatalytic purification	Strong UV absorber; multiple crystalline forms	Catalytically oxidizes NO to NO_2 and organics to CO_2	35-54
Carbon Nanotubes (CNT) and Fullerenes	CNT: crystalline; fullerenes: C_{20} –C_{70}	Energy storage; composite materials; drug delivery	CNTs tube-like structure; Fullerenes cage-like	Oxidation of fullerenes in gas phase w/O_2, O_3	55-71
Zero-valent iron (n-ZVI)	Fe^0; $Fe(C_5H_5)_2$ – (ferrocene)	Remediation of groundwater and soil; fuel catalyst	$Fe(C_5H_5)_2$ combusted to n-ZVI; metallic aggregates 20-200 nm	$Fe^0 + O_2 \rightarrow$ Fe(II); Fenton chemistry $\rightarrow$ Fe(III)	72-79
Silver nanoparticles (n-Ag)	n-Ag^0	Antimicrobial/antibacterial additive to consumer products	nAg capped w/stabilizing agents; emitted particles 5-50 nm	Ag coated by organics; agglomeration; oxidant rxns	80-85

Table 2. Sampling methods for nanoparticles of importance for environmental considerations.

Collection Method	Major Use	Size range	Advantages	Disadvantages	References
Conventional filtration (with size-cutoff inlet)	Collection for bulk analytical methods	< 10 μm depending on aerosol inlet	Straightforward; large sampling volumes	Difficulty separating ENPs from INPs	54
Electrostatic precipitation (includes DC[a] and PC[a])	Electric field used to maintain NP morphological integrity	Varied depending on applied field	Low pressure drops; high collection efficiency for NP	Low volumes sampled; low mass for analytical methods	48, 74, 84, 94, 95, 96-98
Thermophoretic precipitation (TP)	NP size distributions and number concentrations by microscopy	< 100 nm	Efficient means to direct NPs to TEM grid	Limited analytical uses	42, 45, 56, 76, 87, 96, 99, 100
Impaction (includes low volume impactor; LPI)	Collect PM in absence of filtering material	50 – 10,000 nm	Simple approach for size segregated methods	Small sample volumes; Inefficient for high size cuts	74, 75, 88,103-105
MOUDI[b] (conventional)	Multiple micron size ranges for bulk analysis or microscopy	0.05, 0.1, 0.32, 0.56, 1.0, 1.8, 3.2, 5.6, 10, 18 μm	High size separation in micron range for analysis	Large pressure drops; Disruption of NP agglomerates	104-105
MOUDI[b] (nano)	Multiple nano sized ranges for bulk analysis or microscopy	10, 18, 32, 56, 100 nm	High size separation in nano range for analysis	Large pressure drops; Disruption of NP agglomerates	101-103
Differential mobility analyzer (DMA)	Particle number, surface area, volume concentration	20 – 1000 nm	Extremely fine particle sizing in micron range	Insufficient mass for most chemical analysis methods	75, 95, 102
Nano-DMA	Particle number, surface area, volume concentration	2 – 100 nm	Extremely fine particle sizing in nm range	Insufficient mass for most chemical analysis methods	75, 95, 102, 106, 107
Parallel-flow diffusion battery (PFDB)	Multiple size ranges for bulk analysis or microscopy	Eight size bins < 700 nm	Direct collection on filters or TEM grid	Limited size bins in the nano range	108-110

[a] DC – Diffusion charging; PC – Photoelectric charging

[b] MOUDI – Micro-orifice, uniform-deposit impactor

Table 3. Current and potential methods for detecting nanoparticles of importance in environmental measurements.[a]

Analytical technique	Operating Principle	Detection Method	Size range (nm)	Measurement Time Scale	References
Scanning mobility particle sizer (SMPS)	Electrostatic classification	Optical particle counting	20 – 1000 (conventional) 2 – 100 (nano)	Minutes (min)	75, 95, 102, 111-118
Engine exhaust particle sizer (EEPS)	Electrostatic classification	Electrometer	20 – 500	Millisecond	105, 115, 122
Fast mobility Particle sizer (FMPS)	Electrostatic classification	Electrometer	20 – 500	Millisecond	105, 115, 122
Inductively coupled plasma – mass spectroscopy (ICP-MS)	Atomic ionization by plasma energy	Mass spectrometer	Collection device dependent	Bulk analysis	57, 75. 103, 107, 123
Atomic absorption spectroscopy (AAS)	Absorption of UV, visible, IR radiation	Photomultiplier, phototube	Collection device dependent	Bulk analysis	101
Elemental carbon/Organic carbon analysis (EC-OC)	Oxidize aerosol carbon to CO_2	Thermo-optical	< 1000	Bulk analysis	104, 105, 124
X-ray fluorescence (XRF)	Element absorbs then fluoresces X-rays	Energy-dispersive solid-state detector	Collection device dependent	Bulk analysis	54
X-ray absorption spectroscopy (XAS)	Absorption of X-rays by oxidized element	Photomultiplier or solid-state detector	Collection device dependent	Bulk analysis	47, 130
Scanning electron microscopy (SEM)	Electron microscopy imaging	Scintillator-photomultiplier, semiconductor	1 – 100	Filter or grid collection for off-line measurement of particles	89, 129
Transmission electron microscopy (TEM)	Electron transmission and imaging	Scintillator-photomultiplier, semiconductor	0.05 – 100	Grid collection for off-line measurement of particles	45, 54, 89, 95, 117, 131, 132
Energy dispersive spectroscopy (EDS)	Electron excitation and X-ray emission	Energy-dispersive solid-state detector	1 – 100 (SEM) 0.05 – 100 (TEM)	Filter or grid collection for off-line measurement of particles	22, 74, 91, 92, 133
X-ray diffraction (XRD)	Diffraction of X-rays from atomic spacing	Electrometer	Collection device dependent	Filter collection for off-line measurement of particles	42, 54, 56, 80
Scanning probe microscopy (SPM)	Electric current between probe and sample	Electrometer	Collection device dependent	Probe collection for off-line measurement of particle	135-139
Single particle mass spectroscopy (SPMS)	Size separation / flash heating of single particle	Electron ionization	10 – 1000	Scan: min Selected ion: sec	75, 132, 140-143

[a] Bulk analysis typically achieved by filter collection.

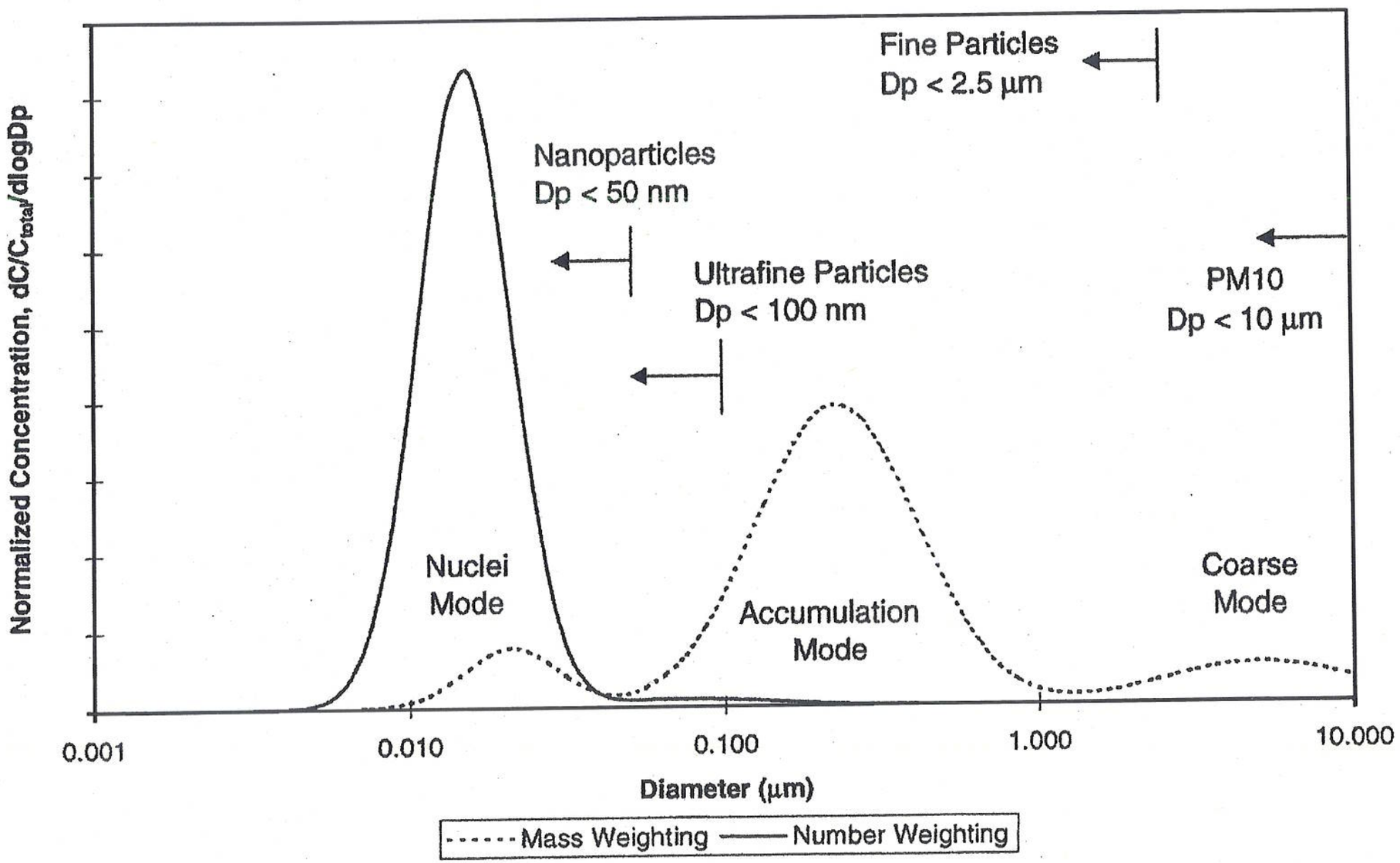
Fine Particles
Dp < 2.5 µm
Nanoparticles
Dp < 50 nm
Ultrafine Particles
Dp < 100 nm
PM10
Dp < 10 µm
Nuclei
Mode
Accumulation
Mode
Coarse
Mode
Normalized Concentration, dC/C_total/dlogDp
0.001
0.010
0.100
1.000
10.000
Diameter (µm)
Mass Weighting
Number Weighting